Geothermometry and geobarometry of high-grade rocks: a case study on garnet–pyroxene granulites in southern Sri Lanka

S. FAULHABER AND M. RAITH

Mineralogisch-Petrologisches Institut, Universität Bonn, Poppelsdorfer Schloss, 5300 Bonn, FRG

Abstract

In the central granulite belt of Sri Lanka, garnet–pyroxene granulites of granitic and gabbro–noritic composition are the most abundant rock types. The micro-structures and mineral chemistry data prove complete attainment of textural and large-scale chemical equilibrium during and following a phase of extreme penetrative deformation at conditions of the granulite facies (800–850 °C, 5 to 9 kbar). On a local scale, especially along the intergranular system, continued cation exchange decoupling from the early ceasing net-transfer reactions destroyed the near-peak metamorphic equilibrium. The extreme compositional variation of the coexisting ferro-magnesian phases (Fe/(Fe + Mg): gar 0.98–0.65, opx 0.92–0.40, cpx 0.88–0.28) and the near-isothermal conditions of equilibration throughout the studied area enabled examination of the effects of non-ideal mixing in garnet and pyroxenes on the equilibrium constants of reactions used in geothermobarometry, and tests on the quality of commonly applied thermometers/barometers and the validity of activity models adopted in the calibrations. The Sri Lankan data set reveals more or less pronounced compositional dependences for all of the tested gar–opx/gar–cpx Fe–Mg exchange thermometers and the opx + plg $\rightleftharpoons$ gar + qtz barometers. Evidently the recommended solution models do not adequately describe the mixing properties of the involved ferro-magnesium mineral phases (garnet, orthopyroxene and clinopyroxene).

KEYWORDS: geothermometry, geobarometry, garnet, pyroxene, granulite, Sri Lanka.

Introduction

A MAJOR problem in the geothermobarometric analysis of *P–T* regimes in metamorphic terranes is related to the equilibrium state of the rocks. In high-grade amphibolite to granulite facies terranes complete textural and chemical equilibrium is commonly attained during near-peak metamorphic recrystallization, especially when the rocks have been strongly affected by penetrative deformation. However, on the way back to surface, during decompression and cooling, the 'large-scale' chemical equilibrium in the high-grade assemblages is destroyed to variable extent by continued inter-crystalline cation exchange decoupling from the early-ceasing net-transfer reactions, by exsolution processes and hydration. Re-equilibration is incomplete, of small range and mainly confined to 'small-scale' near grain boundary domains. At best, mosaic-type equilibrium is attained in numerous intergranular subsystems of specific mineralogy and chemical composition. Yet, because of the differential kinetics of the retrograde reactions and the variable sensitivity of the mineral phases to retrogression, chemical equilibrium may never be achieved in these domains. It stands to reason, that in order to constrain with reliance the near-peak metamorphic conditions and the retrograde *P–T* path, the effects of retrogression on the micro-textures and equilibrium compositions of the coexisting mineral phases must be evaluated with great care. Unfortunately this aspect is too often neglected in petrologic studies on high-grade rocks.

A problem of similar importance in the thermobarometric analysis of *P–T* regimes concerns the quality of calibrations of geothermometers and geobarometers and, most important, the modelling of activity–composition relations for the involved mineral phases. The calibration of temperature-sensitive cation exchange equilibria and especially of pressure-sensitive net-transfer reactions applicable to garnetiferous granulites

Mineralogical Magazine, March 1991, Vol. 55, pp. 33–56

has made considerable progress in the last decade (cf. Berman, 1988; Powell and Holland, 1985; Holland and Powell, 1990). Nevertheless, uncertainties in the application to natural rocks result from the fact that most of the available models have to be applied outside the pressure–temperature ranges and composition spaces of their calibration and the adopted activity models may not adequately describe the mixing properties of the multi-component natural solid solutions.

To illustrate and investigate this set of problems, the Proterozoic granulite terrane of Sri Lanka is ideally suited. Within a rather small crustal domain, a variety of magmatic and sedimentary rock types occur which are sensitive to changes in metamorphic pressure, temperature and fluid composition. They experienced a common well-constrained tectono–metamorphic history culminating in a prolonged stage of static recrystallization at granulite facies conditions. The multiphase assemblages of widespread garnetiferous granulites allow tests on the various formulations of a maximum number of geothermometers and geobarometers involving garnet, pyroxenes, amphibole, biotite, feldspars, quartz and opaque mineral phases. The wide compositional range of these rocks from granitic to gabbro–noritic with pronounced variations of Fe/(Fe + Mg) enables examination of the effects of bulk chemistry on the composition of coexisting mineral phases at defined P–T conditions and, most important, investigation of the validity of activity models for the multicomponent solid solutions adopted in the various geothermobarometric formulations. Last but not least, the examination of compositional systematics reflecting regional gradients of the near-peak metamorphic P–T regime, the effects of bulk rock chemistry as well as of retrograde local re-equilibration can be based on a comprehensive set of observations and mineral chemistry data from a large number of rock specimens.

Geological setting

The Precambrian basement of Sri Lanka—a small fragment of the Gondwana supercontinent—exposes a substantial section of the lower continental crust with a large diversity of amphibolite to granulite grade rocks. Based on lithology, structure and metamorphic features three major rock units have been identified (cf. Katz, 1971; Corray, 1978; Vitanage, 1985 (Fig. 1).

(1) The *Highland Series* and the lithologically similar *South-West Group* constituting a NS-trending linear mobile belt through the central and southern parts of the island which is predominantly composed of granulite-grade metasediments (gar-sill gneisses, gar-cord-sill gneisses, garnetiferous quartzo-feldspathic gneisses, quartzites, marbles and calc-silicate rocks) intimately interbanded with basaltic to rhyolitic metavolcanic rocks (gar-pyx-hbl granulites, charnockites) and pre- to syntectonic granitoid intrusives. Recent isotope data indicate a derivation of the clastic sediments mainly from late Archaean continental source terranes (Nd model age data of 3.2 to 2.0 Ga, Milisenda *et al.*, 1988) and the deposition of the entire supracrustal assemblage before about 1.9 Ga (U-Pb zircon data on granitoids; Hölz and Köhler, 1989);

(2) The amphibolite-grade gneiss terrane of the *Eastern Vijayan Complex* flanking the central granulite belt in the east and southeast along a major tectonic suture. The I-type granitoid characteristics and late Proterozoic Nd model ages of the dominant tonalitic to granodioritic hlb-bio gneisses and migmatites together with the present-day tectonic setting prompted Milisenda *et al.* (1988) to interpret the Eastern Vijayan Complex as a late Proterozoic Andean-type magmatic arc which was welded to the older granulite terrane as a result of Panafrican collisional tectonics;

(3) The amphibolite-grade terrane of the *Western Vijayan Complex* dominated by an assemblage of interbanded granitic gneisses, biotite gneisses and migmatites intruded by pink granites, and bordering the central granulite belt in the west along an ill-defined boundary. The Western Vijayan Complex including the lithologically similar series of the *Arena Synforms* form the structurally highest crustal units in the basement of Sri Lanka. The Nd model age data and U–Pb zircon data obtained for orthogneisses and metasediments (Milisenda *et al.*, 1988; Hölzl and Köhler, 1989) identify both units as Mid-Proterozoic (2.0–1.3 Ga) juvenil additions to the crust which most likely were thrusted as a major nappe onto the older granulite terrane during Panafrican collisional tectonics.

High-grade metamorphism in the central granulite belt occurred during and outlasted at least two phases of tight isoclinal folding and significant thrusting (cf. Berger and Jayasinghe, 1976; Sandiford *et al.*, 1988). Recent Sm–Nd garnet–whole-rock data and U–Pb zircon and monazite data (600 to 500 Ma; Hölzl and Köhler, 1989) indicate a Panafrican age of metamorphism which is also the time of late synorogenic granite intrusions. Intense flattening and NS-directed

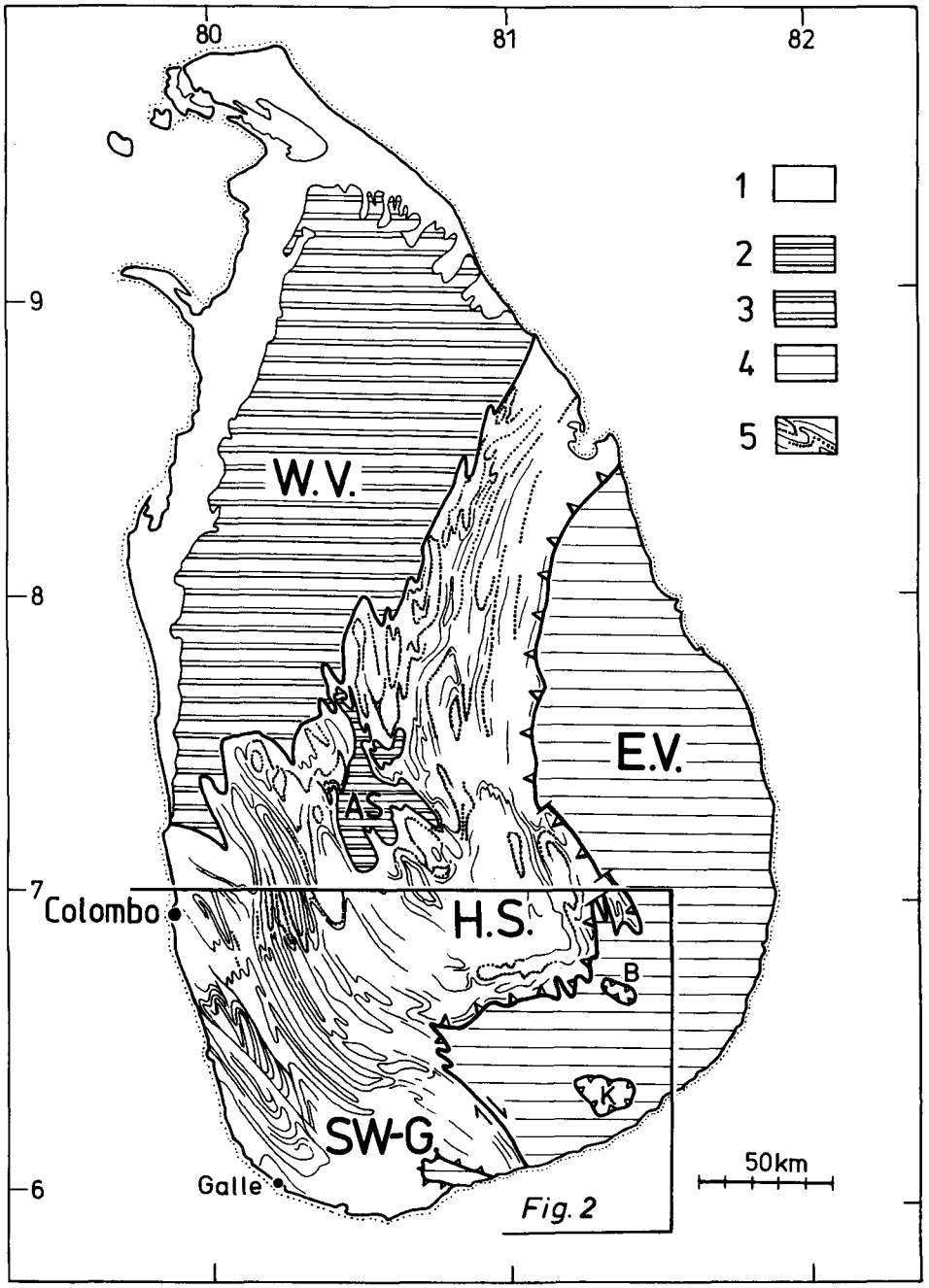

FIG. 1. Geological sketch map of Sri Lanka showing the major litho-tectonic units (adopted from Cooray, 1978): 1, Phanerozoic cover; 2, synform structures of the Arena Series (A.S.); 3, Western Vijayan Complex (W.V.); 4, Eastern Vijayan Complex (E.V.); 5, the central granulite belt with the Highland Series (H.S.) and the South-West Group (SW-G.). Within the central granulite belt foliation trends and quartzite bands (stippled lines) are shown to illustrate schematically the general structural pattern. K and B are the Kataragama and Buttala tectonic klippen of Highland Series granulites within the amphibolite grade gneiss terrane of the Eastern Vijayan Complex.

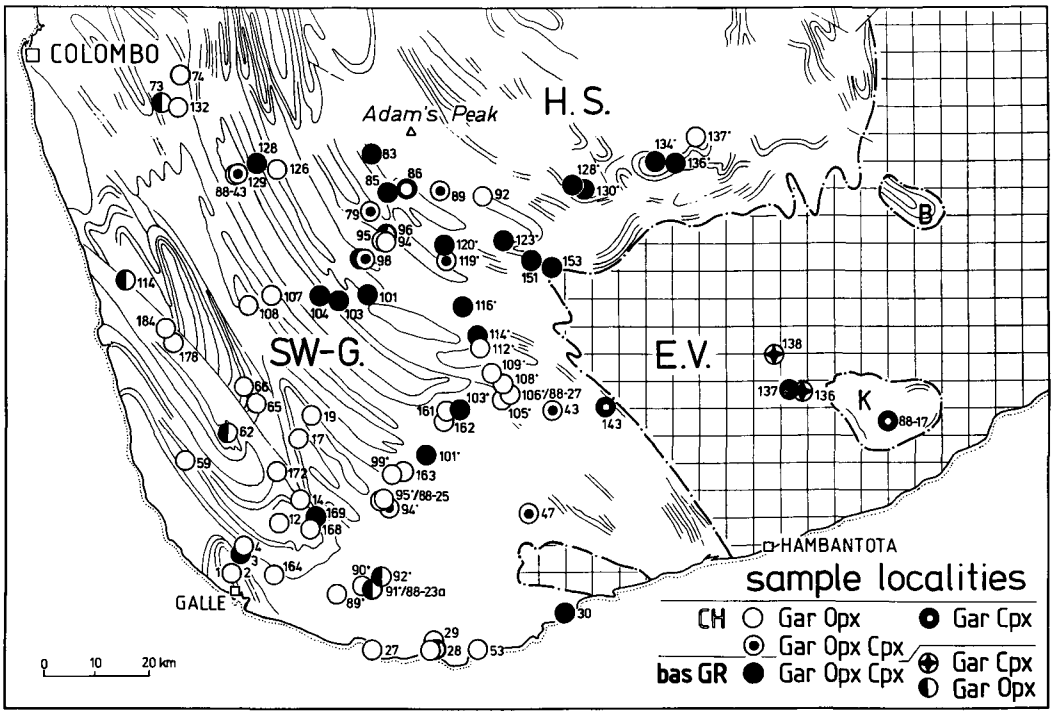

FIG. 2. Sketch map of southern Sri Lanka showing the localities of garnet–pyroxene granulite samples studied in this paper. Changes in the charnockite paragenesis can be related to the strongly pressure dependent reaction opx + plg $\rightleftharpoons$ gar + cpx + qtz and document a pronounced regional gradient in paleo-pressure: lowest pressures (gar + opx) in the structurally highest western part of the central granulite belt, medium pressures (gar + opx + cpx) at mid-tectonic levels and highest pressures (gar + cpx) near the thrust-contact to the Eastern Vijayan basement complex and within the Kataragama klippe. CH = charnockites, bas GR = basic granulites; samples numbers with '·' are prefixed SL, others have the prefix BSL.

stretching led to the development of prominent linear and planar fabrics especially in the quartzo–feldspathic granulites and was outlasted by wholesale recrystallization at conditions of the granulite facies. During these phases of horizontal thrust-tectonics, the Western Vijayan Complex and central granulite belt were welded together and thrusted onto the Eastern Vijayan Complex. Subsequent open folding with the formation of NS-trending wide-scale synform and antiform structures postdated the main granulite facies event. Due to the absence of wide-scale penetrative deformation, as evidenced by the lacking axial plane fabrics the micro-structures and assemblages of the granulites experienced only minor modifications. Rb–Sr biotite whole-rock data range between 485 to 405 Ma and could either indicate an extended period of slow cooling following the peak of granulite facies metamorphism or a later thermal event (Hölzl and Köhler, 1989).

Garnet–pyroxene granulites: assemblages and phase relations

The following discussion of geothermobarometric aspects is based on a detailed petrological study of garnet and pyroxene-bearing granulites from the southern part of Sri Lanka (Faulhaber, 1991). Assemblages and selected mineral chemistry data for 86 samples considered in this study are summarized in Tables 1 and 2. Sample localities are given in a simplified map showing the main structural trends in the granulite terrane of the South-West Group and the Highland Series (Fig. 2). According to their mineralogy and bulk chemistry, two major rock types are distinguished—charnockites and basic granulites.

The *charnockites* are characterized by granitic composition and high Fe/(Fe + Mg) ratios (Fig. 3). Depending on the paleo–pressure regime which closely correlates with the tectonic structure of the terrane (Fig. 16), the following typical silicate assemblages are developed:

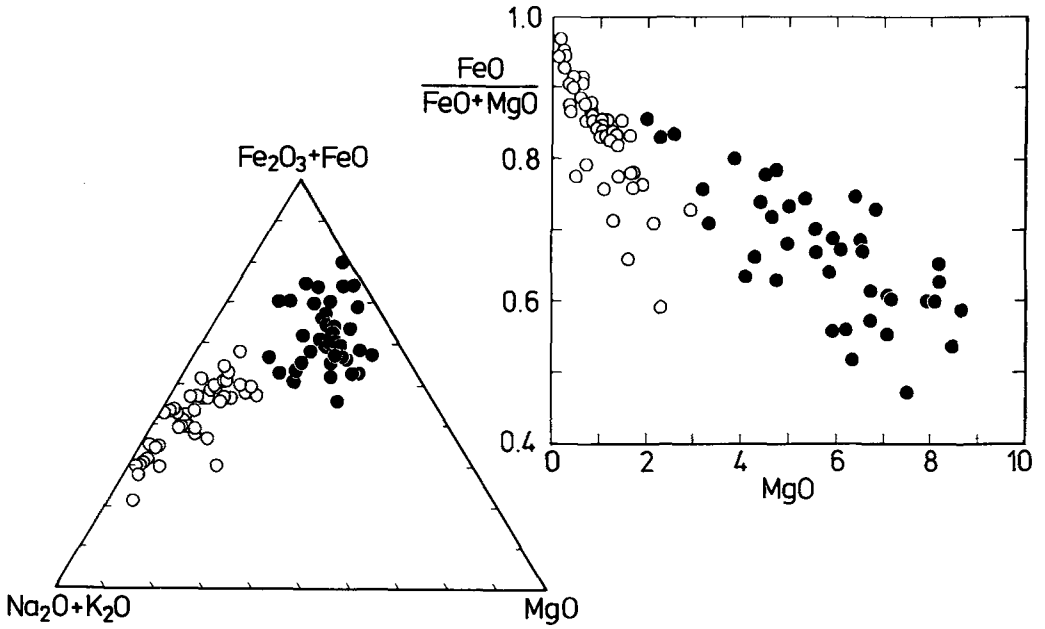

FIG. 3. Alk-F-M diagram illustrating the bimodel character of garnet–pyroxene granulites in the southwestern part of Sri Lanka. The FeO/(FeO + MgO) *vs.* MgO diagram (wt. %) documents the contrasting X_{Fe} compositions of charnockites (circles) and basic garnetiferous granulites (dots).

gar + opx + plg + kf + qtz ± hbl, bio
low to medium P
gar + fa + cpx + plg + kf + qtz ± hbl, bio
low P; very rare,
≫Fe/(Fe + Mg)
gar + opx + cpx + plg + kf + qtz ± hbl, bio
medium P
gar + cpx + plg + kf + qtz ± hbl, bio
high P

The *basic granulites* have tholeiitic compositions, with lower Fe/(Fe + Mg) ratios (Fig. 3). The following typical silicate assemblages are developed, the garnet-bearing assemblages occurring exclusively in the regions of medium to high paleo-pressures:

gar + opx + hbl + plg ±bio, qtz, kf
gar + opx + cpx + hbl + plg ±bio, qtz, kf
gar + cpx + hbl + plg ±bio, qtz, kf
opx + cpx + hbl + plg ±bio, qtz, kf
opx + hbl + plg ±bio, qtz, kf
cpx + hbl + plg ±bio, qtz, kf

The ferro-magnesian phases of charnockites and basic granulites show extensive compositional variation which to a large extent is controlled by the Fe/(Fe + Mg) ratio of the rocks: garnet (X_{Fe} = 0.65–0.98), orthopyroxene (X_{Fe} = 0.40–0.92), clinopyroxene (X_{Fe} = 0.28–0.88), hornblende (X_{Fe} = 0.37–0.85) and biotite (X_{Fe} = 0.25–0.72).

Garnet in the basic granulites is saturated in grossular component with a systematic yet small increase towards more Fe-rich solid solutions ($X_{Ca} : X_{Fe} = 0.17 : 0.65 \rightarrow 0.21 : 0.87$), (Fig. 4).

In the clinopyroxene-free charnockite assemblage, grossular content in garnet continuously increases with paleo-pressure until, at high pressures, saturation is attained (X_{Ca} = 0.18) (Fig. 5). Clinopyroxene may then appear in the charnockite assemblages (Fig. 4). This compositional effect is accompanied by a systematic rotation of the opx–gar tie-lines towards more iron-rich compositions. The increasing slope of the tie-lines with increasing grossular content is reflected by the systematic variation in $\ln K_D$ (Fig. 5). It documents the non-ideality effect of grossular component on the mixing properties of the ternary Fe–Mg–Ca garnets (cf. Ganguly and Saxena, 1984), and consequently on the Fe–Mg exchange equilibrium between garnet and orthopyroxene. In the orthopyroxene-free charnockite assemblages, garnets have the highest grossular contents.

The observed compositional trends in the ferromagnesian phases and the concomitant changes of the charnockite assemblages in addition to the pronounced effects of bulk rock chemistry, are

Table 1. Compositional data of coexisting garnet, orthopyroxene, clinopyroxene and plagioclase, in charnockites and basic granulites of southern Sri Lanka (core compositions of isolated phases and coarse-grained contact phases).

garnet => $X_{Fe} = Fe^{2+} / (Fe^{2+} + Mg + Ca + Mn)$

$X_{Mg} = Mg / (Fe^{2+} + Mg + Ca + Mn)$

$X_{Ca} = Ca / (Fe^{2+} + Mg + Ca + Mn)$

pyroxene => $X_{Fe} = Fe^{2+} / (Fe^{2+} + Mg)$

plagioclase => $X_{Ca} = Ca / (Ca + Na + K)$

BASIC GRANULITES - compositional data

SAMPLES	GARNET			OPX	CPX	PLG
	X_{Ca}	X_{Fe}	X_{Mg}	X_{Fe}	X_{Fe}	X_{Ca}
SL 90-3	0.211	0.622	0.138	-	0.470	0.563
BSL 88-23a	0.183	0.611	0.175	0.523	-	0.537
SL 92-2	0.111	0.716	0.147	0.596	-	0.363
SL 101-2	0.192	0.626	0.149	0.554	0.456	0.456
SL 103-1	0.188	0.568	0.210	0.471	0.349	0.463
SL 114-1	0.183	0.562	0.237	0.437	0.290	0.578
SL 116-1	0.192	0.630	0.153	0.570	0.450	0.410
SL 120-1	0.195	0.641	0.143	0.578	0.500	0.389
SL 123-1	0.173	0.537	0.271	0.417	0.271	0.478
SL 126-1	0.188	0.652	0.132	0.567	0.431	0.328
SL 128-1	0.189	0.590	0.195	0.481	0.358	0.447
SL 130-1	0.185	0.570	0.220	0.471	0.304	0.659
SL 134-1	0.184	0.627	0.167	0.552	0.381	0.359
SL 136-1	0.193	0.623	0.166	0.549	0.437	0.361
BSL 3-2	0.196	0.632	0.149	0.603	0.451	0.906
BSL 28-3	0.179	0.615	0.163	0.561	-	0.482
BSL 30-3	0.194	0.633	0.152	0.560	0.434	0.354
BSL 62-3	0.067	0.647	0.261	0.492	-	0.790
BSL 73-4	0.083	0.697	0.185	0.555	-	0.379
BSL 83-2	0.175	0.535	0.266	0.413	0.263	0.475
BSL 85-1	0.184	0.560	0.201	0.483	0.347	0.462
BSL 85-2	0.181	0.575	0.200	0.485	0.375	0.430
BSL 96-1	0.189	0.574	0.205	0.473	-	0.484
BSL 98-3	0.185	0.595	0.186	0.506	0.366	0.411
BSL 101-1	0.194	0.589	0.185	0.525	0.412	0.485
BSL 103-1	0.188	0.577	0.215	0.480	0.350	0.517
BSL 104-1	0.199	0.660	0.111	0.653	0.541	0.446
BSL 114-3	0.076	0.737	0.161	0.621	-	0.391
BSL 128-1	0.194	0.639	0.136	0.595	0.456	0.496
BSL 128-2	0.204	0.657	0.104	0.669	0.535	0.489
BSL 136-1	0.218	0.533	0.219	-	0.305	0.367
BSL 137-1	0.198	0.591	0.190	0.516	0.360	0.320
BSL 138-2	0.243	0.523	0.211	-	0.305	0.424
BSL 151-2	0.174	0.550	0.249	0.414	0.286	0.438
BSL 153-1	0.171	0.522	0.272	0.391	0.326	0.355
BSL 169-1	0.202	0.675	0.103	0.705	0.593	0.874

CHARNOCKITES - compositional data

SAMPLES	GARNET			OPX	CPX	PLG
	X_{Ca}	X_{Fe}	X_{Mg}	X_{Fe}	X_{Fe}	X_{Ca}
SL 89-1	0.166	0.757	0.041	0.851	-	0.363
SL 94-1	0.205	0.750	0.024	0.914	0.867	0.288
BSL 88-25c	0.197	0.695	0.086	0.698	-	0.405
BSL 88-25d	0.192	0.702	0.078	0.729	-	0.375
SL 99-1	0.187	0.694	0.091	0.715	-	0.380
SL 106-1	0.197	0.683	0.104	0.663	-	0.340
BSL 88-27a	0.187	0.686	0.109	0.678	-	0.313
SL 108-1	0.195	0.673	0.113	0.646	-	0.350
SL 109-2a	0.205	0.688	0.086	0.696	-	0.314
SL 112-1a	0.190	0.740	0.044	0.826	-	0.223
SL 119-2	0.208	0.707	0.037	0.843	0.776	0.212
SL 137-1	0.192	0.660	0.120	0.586	-	0.284
BSL 1-1	0.123	0.758	0.098	0.705	-	0.385
BSL 2-2	0.046	0.723	0.198	0.569	-	0.302
BSL 4-1	0.086	0.788	0.093	0.746	-	0.329
BSL 4-2	0.083	0.781	0.108	0.738	-	0.299
BSL 12-1	0.119	0.751	0.097	0.681	-	0.472
BSL 14-1	0.074	0.731	0.185	0.573	-	0.296
BSL 17-2	0.131	0.746	0.103	0.722	-	0.387
BSL 19-1	0.149	0.750	0.084	0.746	-	0.362
BSL 27-1	0.198	0.740	0.040	0.849	-	0.340
BSL 28-2	0.201	0.678	0.097	0.682	-	0.397
BSL 43-1	0.211	0.726	0.041	0.824	0.732	0.228
BSL 47-1	0.201	0.703	0.075	0.726	0.592	0.302
BSL 53-4	0.194	0.661	0.097	0.651	-	0.327
BSL 59-1	0.081	0.781	0.109	0.703	-	0.336
BSL 65-1	0.048	0.699	0.239	0.514	-	0.319
BSL 66-1	0.079	0.757	0.143	0.638	-	0.357
BSL 74-1	0.085	0.642	0.228	0.498	-	0.429
BSL 79-3	0.193	0.655	0.120	0.664	0.569	0.227
BSL 89-1	0.199	0.650	0.109	0.632	0.538	0.328
BSL 92-1	0.188	0.630	0.166	0.551	-	0.371
BSL 94-1	0.186	0.711	0.067	0.781	-	0.254
BSL 95-3	0.118	0.717	0.132	0.650	-	0.233
BSL 98-1	0.191	0.712	0.078	0.742	0.631	0.288
BSL 107-1	0.210	0.725	0.041	0.844	-	0.351
BSL 108-2	0.114	0.706	0.153	0.609	-	0.445
BSL 126-1	0.192	0.697	0.083	0.722	-	0.397
BSL 129-1	0.246	0.696	0.024	0.909	0.871	0.300
BSL 88-43-1	0.225	0.713	0.022	0.939	0.833	0.316
BSL 88-43-3	0.186	0.706	0.074	0.760	-	0.346
BSL 132-3	0.088	0.696	0.173	0.583	-	0.395
BSL 143-2	0.208	0.747	0.030	-	0.820	0.217
BSL 161-3	0.188	0.682	0.108	0.660	-	0.368
BSL 163-1	0.176	0.722	0.079	0.742	-	0.336
BSL 164-1	0.059	0.751	0.143	0.660	-	0.203
BSL 168-1	0.107	0.782	0.087	0.734	-	0.348
BSL 178-1	0.082	0.768	0.121	0.631	-	0.375
BSL 184-1	0.065	0.732	0.179	0.585	-	0.314
BSL 88-17	0.264	0.689	0.023	-	0.874	0.094

Table 2. Mineral assemblages of charnockites and basic granulites of southern Sri Lanka.

Table 2: BASIC GRANULITES - mineral assemblages

Samples	Mineral Phases							
SL 90-3	Gra-	Cpx-		Hbl-	<Bio-			Plg, Opaques
BSL 88-23a	Gra-		Opx-	Hbl-				Plg, Opaques
SL 92-2	Gra-		Opx-			<Qtz-	<<Kf-	Plg, Opaques
SL 101-2	Gra-	Cpx-	Opx-	Hbl-				Plg, Opaques
SL 103-1	Gra-	Cpx-	Opx-	Hbl-				Plg, Opaques
SL 114-1	Gra-	Cpx-	Opx-	Hbl-				Plg, Opaques
SL 116-1	Gra-	Cpx-	Opx-	Hbl-	<Bio-			Plg, Opaques
SL 120-1	Gra-	Cpx-	Opx-	<Hbl-		Qtz-		Plg, Opaques
SL 123-1	Gra-	Cpx-	Opx-	Hbl-				Plg, Opaques
SL 126-1	Gra-	Cpx-	Opx-	Hbl-	Bio-			Plg, Opaques
SL 128-1	Gra-	Cpx-	Opx-	Hbl-	<Bio	Qtz-		Plg, Opaques
SL 130-1	Gra-	Cpx-	Opx-	Hbl-	<Bio-			Plg, Opaques
SL 134-1	Gra-	Cpx-	Opx-	Hbl-	<Bio		<<Kf-	Plg, Opaques
SL 136-1	Gra-	Cpx-	Opx-	Hbl-		<Qtz-		Plg, Opaques
BSL 3-2	Gra-	Cpx-	Opx-	Hbl-				Plg, Opaques
BSL 28-3	Gra-		Opx-	Hbl-	Bio-			Plg, Opaques
BSL 30-3	Gra-	Cpx-	Opx-	Hbl-	Bio-			Plg, Opaques
BSL 62-3	Gra-		Opx-		Bio-			Plg, Opaques
BSL 73-4	Gra-		Opx-		Bio-		<<Kf-	Plg, Opaques
BSL 83-2	Gra-	Cpx-	Opx-	Hbl-				Plg, Opaques
BSL 85-1	Gra-	Cpx-	Opx-	Hbl-	<Bio-			Plg, Opaques
BSL 85-2	Gra-	Cpx-	Opx-		<Bio-	Qtz-	<<Kf-	Plg, Opaques
BSL 96-1	Gra-	Cpx-	Opx-	Hbl-				Plg, Opaques
BSL 98-3	Gra-	Cpx-	Opx-	Hbl-	Bio-			Plg, Opaques
BSL 101-1	Gra-	Cpx-	Opx-	Hbl-				Plg, Opaques
BSL 103-1	Gra-	Cpx-	Opx-	Hbl-	Bio-			Plg, Opaques
BSL 104-1	Gra-	Cpx-	Opx-	Hbl-	<Bio-			Plg, Opaques
BSL 114-3	Gra-		Opx-		Bio-	Qtz-	<<Kf-	Plg, Opaques
BSL 128-1	Gra-	Cpx-	Opx-	Hbl-	<Bio-	Qtz-		Plg, Opaques
BSL 128-2	Gra-	Cpx-	Opx-	Hbl-		Qtz-		Plg, Opaques
BSL 136-1	Gra-	Cpx-		Hbl-	<Bio-	Qtz-		Plg, Opaques
BSL 137-1	Gra-	Cpx-	Opx-	Hbl-				Plg, Opaques
BSL 138-2	Gra-	Cpx-	Opx-	Hbl-		Qtz		Plg, Opaques
BSL 151-2	Gra-	Cpx-	Opx-	Hbl-	Bio-			Plg, Opaques
BSL 153-1	Gra-	Cpx-	Opx-	Hbl-	Bio-			Plg, Opaques
BSL 169-1	Gra-	Cpx-	Opx-					Plg, Opaques

Table 2: CHARNOCKITES - mineral assemblages

Samples	Mineral Phases						
SL 89-1	Gar-	Opx-			Bio-	Hbl-	Qtz, Kf, Plg, Opaques
SL 94-1	Gar-	Opx-	Cpx-			<Hbl-	Qtz, Kf, Plg, Opaques
BSL 88-25c	Gar-	Opx-			Bio-	Hbl-	Qtz, Kf, Plg, Opaques
BSL 88-25d	Gar-	Opx-				Hbl-	Qtz, Kf, Plg, Opaques
SL 99-1	Gar-	Opx-			Bio-	Hbl-	Qtz, Kf, Plg, Opaques
SL 106-1	Gar-	Opx-			Bio-	<Hbl-	Qtz, Kf, Plg, Opaques
BSL 88-27a	Gar-	Opx-			Bio-	<Hbl-	Qtz, Kf, Plg, Opaques
SL 108-1	Gar-	Opx-			<Bio-	<Hbl-	Qtz, Kf, Plg, Opaques
SL 109-2a	Gar-	Opx-			<Bio-	Hbl-	Qtz, Kf, Plg, Opaques
SL 112-1a	Gar-	Opx-			<Bio-	Hbl-	Qtz, Kf, Plg, Opaques
SL 119-2	Gar-	Opx-	Cpx-		<Bio-	<Hbl-	Qtz, Kf, Plg, Opaques
SL 137-1	Gar-	Opx-			Bio-	Hbl-	Qtz, Kf, Plg, Opaques
BSL 1-1	Gar-	Opx-			Bio-		Qtz, Kf, Plg, Opaques
BSL 2-2	Gar-	Opx-			Bio-		Qtz, Kf, Plg, Opaques
BSL 4-1	Gar-	Opx-			Bio-		Qtz, Kf, Plg, Opaques
BSL 4-2	Gar-	Opx-			Bio-		Qtz, Kf, Plg, Opaques
BSL 12-1	Gar-	Opx-			Bio-		Qtz, Kf, Plg, Opaques
BSL 14-1	Gar-	Opx-			Bio-		Qtz, Kf, Plg, Opaques
BSL 17-2	Gar-	Opx-			Bio-		Qtz, Kf, Plg, Opaques
BSL 19-1	Gar-	Opx-			Bio-		Qtz, Kf, Plg, Opaques
BSL 27-1	Gar-	Opx-			Bio-	<Hbl-	Qtz, Kf, Plg, Opaques
BSL 28-2	Gar-	Opx-			Bio-	Hbl-	Qtz, Kf, Plg, Opaques
BSL 43-1	Gar-	Opx-	Cpx-			<Hbl-	Qtz, Kf, Plg, Opaques
BSL 47-1	Gar-	Opx-	Cpx-		<Bio-	Hbl-	Qtz, Kf, Plg, Opaques
BSL 53-4	Gar-	Opx-				Hbl-	Qtz, Kf, Plg, Opaques
BSL 59-1	Gar-	Opx-			Bio-		Qtz, Kf, Plg, Opaques
BSL 65-1	Gar-	Opx-			Bio-		Qtz, Kf, Plg, Opaques
BSL 66-1	Gar-	Opx-			<Bio-		Qtz, Kf, Plg, Opaques
BSL 74-1	Gar-	Opx-			Bio-		Qtz, Kf, Plg, Opaques
BSL 79-3	Gar-	Opx-	Cpx-		Bio-	Hbl-	Qtz, Kf, Plg, Opaques
BSL 89-1	Gar-	Opx-	Cpx-		Bio-	Hbl-	Qtz, Kf, Plg, Opaques
BSL 92-1	Gar-	Opx-			<Bio-	Hbl-	Qtz, Kf, Plg, Opaques
BSL 94-1	Gar-	Opx-			<Bio-	<Hbl-	Qtz, Kf, Plg, Opaques
BSL 95-3	Gar-	Opx-			<Bio-		Qtz, Kf, Plg, Opaques
BSL 98-1	Gar-	Opx-	Cpx-				Qtz, Kf, Plg, Opaques
BSL 107-1	Gar-	Opx-			Bio-	Hbl-	Qtz, Kf, Plg, Opaques
BSL 108-2	Gar-	Opx-			Bio-		Qtz, Kf, Plg, Opaques
BSL 126-1	Gar-	Opx-			<Bio-	Hbl-	Qtz, Kf, Plg, Opaques
BSL 129-1	Gar-	Opx-	Cpx-	Ol-	<Bio-	<Hbl-	Qtz, Kf, Plg, Opaques
BSL 88-43-1	Gar-		Cpx-	Ol-		<Hbl-	Qtz, Kf, Plg, Opaques
BSL 88-43-3	Gar-	Opx-				<Hbl-	Qtz, Kf, Plg, Opaques
BSL 132-3	Gar-	Opx-			Bio-		Qtz, Kf, Plg, Opaques
BSL 143-2	Gar-		Cpx-		<Bio-	Hbl-	Qtz, Kf, Plg, Opaques
BSL 161-3	Gar-	Opx-			Bio-	Hbl-	Qtz, Kf, Plg, Opaques
BSL 163-1	Gar-	Opx-			Bio-	Hbl-	Qtz, Kf, Plg, Opaques
BSL 164-1	Gar-	Opx-			Bio-		Qtz, Kf, Plg, Opaques
BSL 168-1	Gar-	Opx-			Bio-	<Hbl-	Qtz, Kf, Plg, Opaques
BSL 178-1	Gar-	Opx-			Bio-		Qtz, Kf, Plg, Opaques
BSL 184-1	Gar-	Opx-			Bio-		Qtz, Kf, Plg, Opaques
BSL 88-17	Gar-		Cpx-		<Bio-	<Hbl-	Qtz, Kf, Plg, Opaques

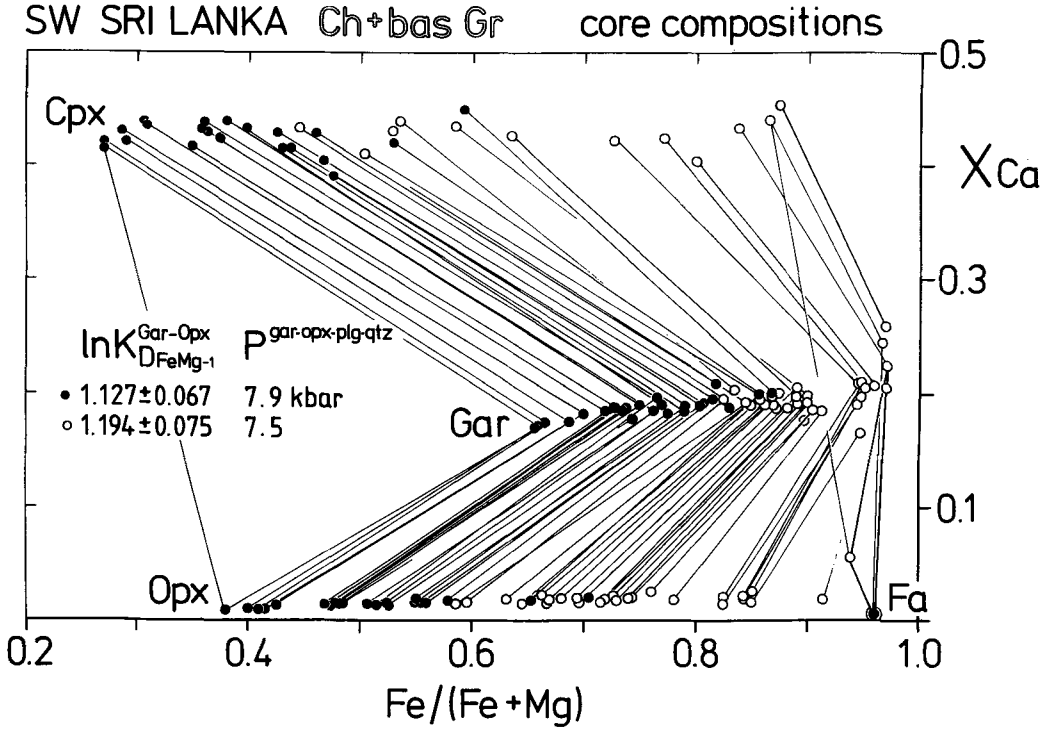

FIG. 4. X_{Fe}–X_{Ca} variations of core compositions of isolated or coarse-grained ferro-magnesian phases in clinopyroxene-bearing charnockites (circles) and basic granulites (dots) characterizing the middle and deepest structural units. In the two-pyroxene paragenesis, grossular content in garnet is buffered with a systematic yet minor increase towards Fe-rich solid solutions. At extreme X_{Fe} bulk compositions the assemblage gar + opx + cpx is replaced by gar + cpx + fa and gar + cpx parageneses.

largely controlled by interaction of the pressure-sensitive net-transfer reactions

orthopyroxene + plagioclase ⇌
$(Fe,Mg)_2Ca$-garnet + quartz

orthopyroxene + plagioclase ⇌
(Fe,Mg)-garnet + clinopyroxene + quartz

and the temperature-sensitive Fe–Mg exchange equilibria. The equilibrium compositions of the coexisting phases attained at near-peak metamorphic recrystallization, however, have been disturbed by decoupling of these reactions during the retrograde stage of metamorphism, as a result of their different kinetics (Faulhaber, 1991).

Systematics of Fe–Mg exchange reactions

To examine the effects of continued retrograde cation exchange between garnet and pyroxenes and the decoupling from the sluggish net-transfer reactions, the mineral phases have been carefully analysed with the microprobe for compositional inhomogeneities and zoning patterns. A graphical representation of the results from selected charnockites and basic granulites may serve to illustrate some important findings (Figs. 6, 7).

Isolated grains of ferro-magnesian phases which are separated from each other by a matrix of feldspar or quartz are almost unzoned and show very little compositional variation within the area of a thin section. This indicates attainment of complete 'large-scale' equilibrium during the thorough syn- to postdeformational recrystallization of the assemblages. Furthermore it is evident that during subsequent cooling and decompression chemical equilibration by net-transfer reactions and cation exchange generally did not continue between the isolated phases. It appears likely, therefore that a fluid phase which could have acted as an efficient intergranular transport medium was not present at this stage. The rare occurrence of coronitic assemblages, on the other hand, shows that under certain circumstances late chemical equilibration was not impossible on a local scale.

Ferro-magnesian phases in contact with each

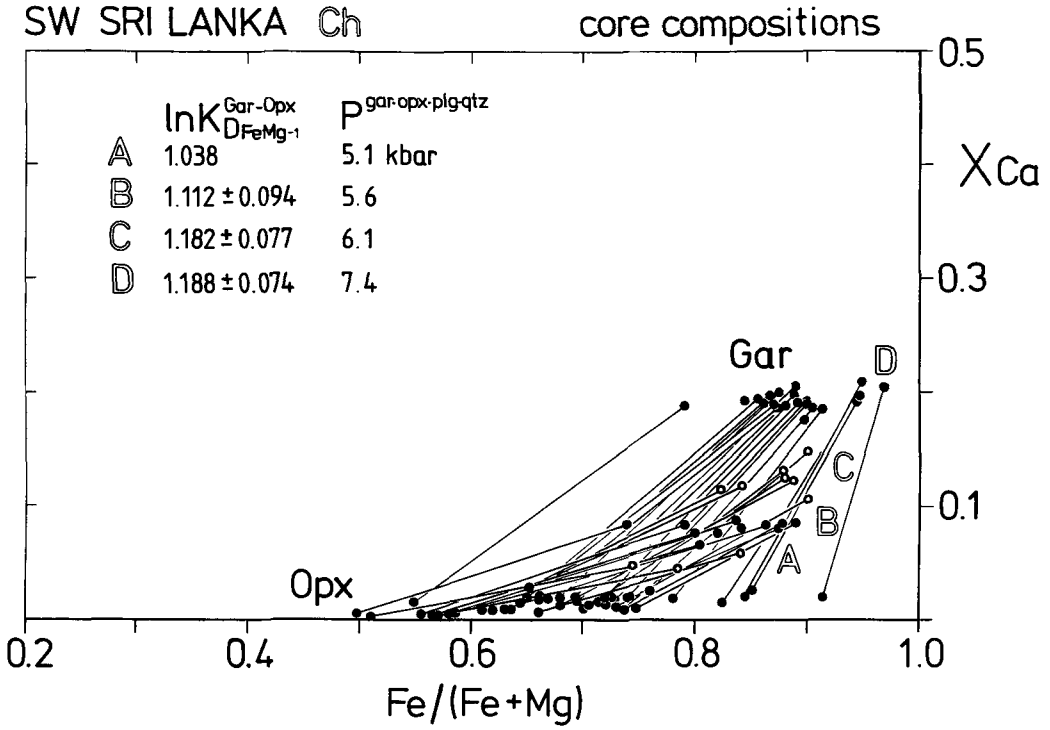

FIG. 5. X_{Fe}–X_{Ca} variations of core compositions of isolated or coarse-grained ferro-magnesian phases in clinopyroxene-free charnockites characterizing the upper to middle structural units of the granulite belt. There is a systematic increase of grossular component in garnet with increasing paleo-pressure (opx + plg $\rightleftharpoons$ gar + qtz barometry; Bhattacharya *et al.*, 1990), until at about 7–8 kbar Ca-saturation is attained. Note that the systematic increase in grossular component correlates with a systematic rotation of the opx–gar tie-lines, i.e. an increase of $\ln K_{DFeMg-1}$ which can be attributed to non-ideal Ca–Mg–(Fe) mixing in the ternary garnet.

other show distinct compositional zoning thus indicating continued cation exchange, whereas in contact with feldspar and quartz compositional zoning is insignificant. These observations prove that retrograde Fe–Mg exchange was only of short range and restricted to the immediate contact zones of ferro-magnesian mineral pairs. Within these domains of local cation exchange, complete chemical equilibrium by net-transfer reactions most likely was not achieved, since modifications of the micro-textures expected to arise from the consumption and growth of the involved mineral phases are not observed. Consequently, pressure estimates obtained from rim compositions using calibrations of pressure-sensitive net-transfer reactions are likely to be erroneous and hence a reliable evaluation of the retrograde *P–T* path is not possible (cf. Frost and Chacko, 1989; Selverstone and Chamberlain, 1990). On the other hand, the temperature estimates derived from the Fe–Mg partitioning data may give meaningful information on the kinetics of retrograde cation exchange and the cooling history of the rocks.

It follows from the preceding discussion that because of the retrograde perturbations of chemical equilibrium, at best the *P–T* conditions of the near-peak metamorphic stage of recrystallization may be determined with confidence using the core compositions of isolated mineral phases.

Stages of the retrograde *P–T* path, in principle, can be assessed for those samples in which coronitic assemblages were formed by the breakdown and neoblastesis of mineral phases during the multivariant pressure-sensitive reaction (Figs. 6, 7)

orthopyroxene + plagioclase $\rightleftharpoons$
(low-*P*/high-*T* paragenesis)
garnet + quartz ± clinopyroxene
(high-*P*/low-*T* paragenesis).

Accordingly, the coarse-grained gar_{II} + qtz_{II} symplectites rimming orthopyroxene in some charnockites could indicate an early stage of

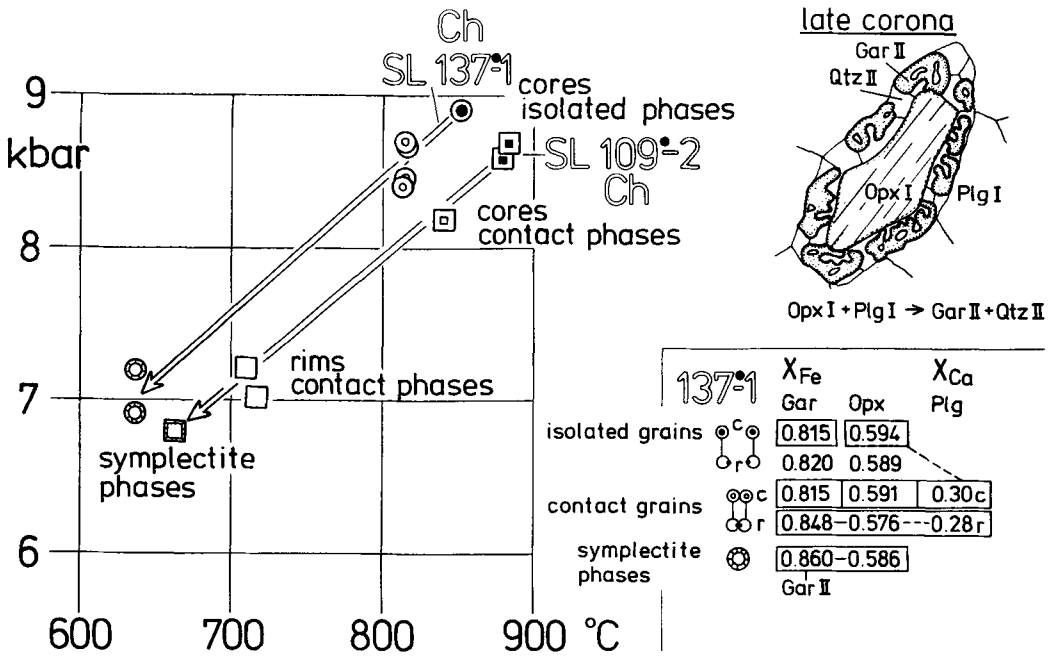

FIG. 6. Pressure–temperature diagram showing the results of gar–opx thermometry and opx + plg ⇌ gar + qtz barometry (calibrations of Bhattacharya *et al.*, 1990) for two selected charnockites. Highest *P–T* estimates are obtained for core compositions of isolated phases which attained complete chemical equilibrium when the highly strained rocks passed through a stage of high-grade thorough recrystallization. Lowest *P–T* conditions on the retrograde *P–T* paths are recorded by the coronitic gar_{II} + qtz_{II} assemblages (upper right). The systematic changes of X_{Fe} compositions of garnet and orthopyroxene due to continued retrograde Fe–Mg exchange is illustrated for sample SL 137°-1.

isobaric cooling, whereas the fine-grained opx_{II} + plg_{II} coronas around garnet in a few basic granulites could be assigned to a late stage of pronounced decompression, an interpretation followed by Schumacher *et al.* (1990) for the Highland Series granulites. Surprisingly the thermobarometric estimates for both corona assemblages based on the composition of the corona phases and the adjacent rims of the breakdown phases, indicate their formation at similar *P–T* conditions on retrograde *P–T* trajectories with essentially the same gradient (Figs. 6, 7). Considering the different *P–T* slopes of the corona-forming reaction in the CMAS and CFAS systems (cf. Perkins and Chipera, 1985, Figs. 1 and 2), the control of corona development by the bulk chemistry of the rocks becomes obvious, and the simultaneous development of the symplectitic assemblages could be explained by cooling and decompression along a common *P–T* path of moderate slope. In the case of the Fe-rich charnockites, the reaction band would have a rather steep slope and hence the retrograde *P–T* trajectory would cross into the high-pressure stability field of the gar + qtz paragenesis, whereas in the case of the Mg-rich basic granulites the *P–T* trajectory would cross the gently sloping reaction band into the low-pressure stability field of the opx + plg paragenesis.

The Fe–Mg distribution data for the cores of isolated mineral phases are plotted in $\ln(Fe/Mg)^{gar}$ versus $\ln(Fe/Mg)^{pyx}$ diagrams (Fig. 8). To minimize the non-ideality effect of grossular component in garnet on the Fe–Mg distribution systematics, only assemblages with buffered garnet composition (X_{Ca} = 0.17–0.21) have been considered. The Fe–Mg partitioning data of mineral pairs which equilibrated at isothermal-isobaric conditions should plot on a straight line with the slope +1, provided the Fe–Mg solid solutions mix ideally or the non-ideality effects in both phases cancel. The systematic deviation of the gar–opx data from the line with the slope +1 can be attributed to non-ideal Fe–Mg mixing of garnet in conformity with recent phase-equilibrium and calorimetric data (Ganguly and Saxena, 1984; Geiger *et al.*, 1987; Berman, 1990), but an additional contribution by non-ideal Fe–Mg mixing in orthopyroxene cannot be ruled out (cf. Chatterjee, 1987; Berman, 1990;

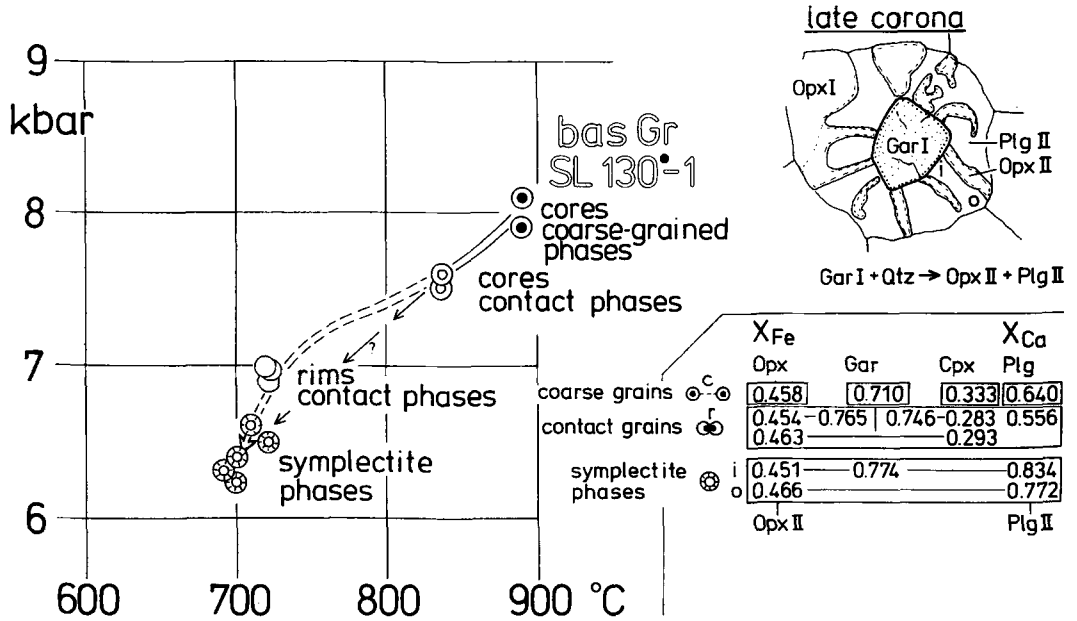

FIG. 7. Pressure–temperature diagram showing the results of gar–opx thermometry and opx + plg ⇌ gar + qtz barometry (calibrations of Bhattacharya *et al.*, 1990) for one selected basic granulite. Highest *P–T* estimates are obtained for the core compositions of the coarse-grained phases and are interpreted to reflect the conditions of the near-peak stage of wholesale recrystallization. In contrast, the lower *T* estimates obtained for cores of small contact phases or contact rims indicate local continuation of retrograde Fe–Mg exchange, whereas the corresponding *P* estimates might have no significance due to the early cessation of net-transfer reactions. A late-stage on the retrograde *P–T* path can be quantified by the coronitic opx_{II} + plg_{II} assemblage (upper right). The systematic change of X_{Fe} compositions due to continued retrograde Fe–Mg exchange is illustrated for the ferro-magnesian phases garnet, orthopyroxene and clinopyroxene (lower right).

Bhattacharya *et al.*, 1990). In contrast, a compositional dependence is not obvious for the gar–cpx data and consequently the non-ideality contributions of both phases apparently cancel (Fig. 8). The effect of non-ideal Fe–Mg mixing on $\ln K_D$ becomes more obvious in Fig. 10. The Fe–Mg partitioning data for the rims of contact phases show the same relationships (Fig. 9).

The relatively small spread of the core data for each of the mineral pairs indicates almost isothermal equilibration of Fe–Mg exchange throughout the southern part of Sri Lanka. Similarly, the small spread of rim data suggests that local Fe–Mg exchange between contact phases was frozen in at uniformly low temperature.

Fe–Mg exchange geothermometry: gar–opx and gar–cpx

The temperature estimates obtained from the core compositions of isolated phases and coarse-grained contact phases with commonly used calibrations of the garnet–pyroxene Fe–Mg exchange geothermometers are compared in Figs. 11 and 12. Again, in order to minimize the effect of varying grossular content on the temperature estimates, only assemblages with buffered garnet composition (X_{Ca} = 0.17–0.21) were considered. Paleo-pressure differences in the order of 3–4 kbar have been neglected and the temperatures were calculated for a constant pressure of 7 kbar. The neglect of a pressure difference up to 4 kbar affects the temperature estimates by only up to 28 °C depending on the applied geothermometer which is in the range of the analytical uncertainties.

The various results of *gar–opx thermometry* are highly discrepant and span the temperature range between 600 and 1050 °C (Fig. 11). However, as stated before, the small spread of the data for the individual calibrations documents near-isothermal Fe–Mg equilibration of garnet and orthopyroxene throughout the studied terrane. The data set is ideally suited to examine the validity of the activity models adopted for the multi-component solid solutions.

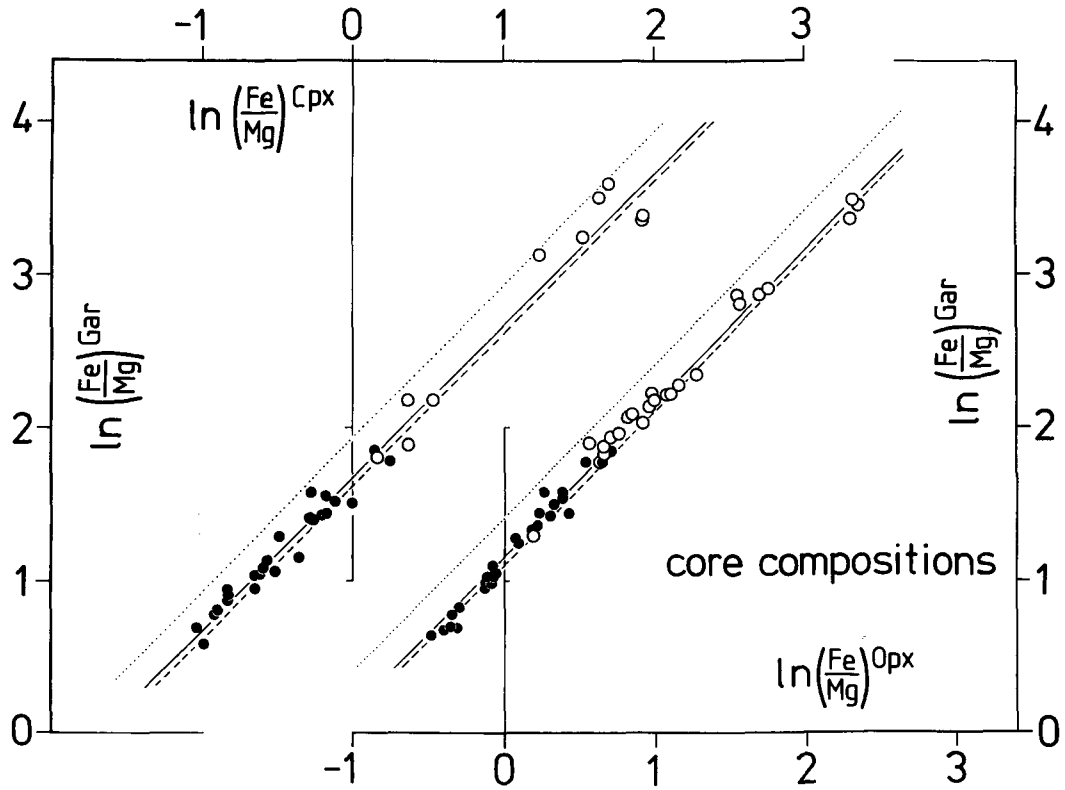

FIG. 8. Representation of Fe–Mg partitioning data (core compositions) for garnet–orthopyroxene and garnet–clinopyroxene pairs in $\ln(Fe/Mg)^{gar}$ vs $\ln(Fe/Mg)^{pyx}$ diagrams. Circles—charnockites; dots—basic granulites. The narrow scatter of the data along lines with +1 slope indicates near isothermal equilibration of the mineral pairs. The stippled lines are linear regressions for core compositions of isolated phases and thus represent the highest equilibration temperature; the dotted lines represent the partitioning data for the rims of contact phases (see Fig. 9) and consequently the lowest equilibration temperature. The slight deviation of the gar–opx data from the +1 slope line indicates effects of non-ideal Fe–Mg mixing. For further discussion see text.

In the formulation of Harley (1984) garnet and orthopyroxene were regarded as ideal Fe–Mg solid solutions and only an excess term to account for the non-ideality effect of the grossular component was introduced in the calibration. It is therefore not surprising that the temperature data derived from Harley's model reflect the compositional dependence of $\ln K_D$. Non-ideal Fe–Mg mixing in garnet and a two-site ideal solution model for orthopyroxene has been adopted in the calibrations of Dahl (1980) and Sen and Bhattacharya (1984). The temperature data show that the compositional effects are either over- or undercorrected. A recent refinement of the thermometer by Bhattacharya *et al.* (1990) in which both garnet and orthopyroxene are considered as non-ideal Fe–Mg solid solutions has not eliminated the compositional dependence, although the model temperatures are in good agreement with average temperature estimates based on phase petrology and oxygen isotope thermometry (Fiorentini *et al.*, 1990; Faulhaber, 1991). Among the tested models only the calibration of Perchuk *et al.* (1985) who attributed the entire compositional effects on $\ln K_D$ to non-ideal mixing in orthopyroxene compensates fairly well the compositional dependence. Their assumption of ideal Fe–Mg mixing in garnet, however, is not justified (cf. Ganguly and Saxena, 1984; Geiger *et al.*, 1987; Berman, 1990; Bhattacharya *et al.*, 1990). Just on the contrary, at high temperatures low-Al orthopyroxenes in good approximation can be described as ideal two-site solutions (cf. Chatterjee, 1987; Berman, 1990). If this holds true for the studied charnockites and basic granulites, the near-isothermal gar–opx partitioning data would only be afflicted with the non-ideality effects of garnet and hence could be used to test the current activity models for the ternary Fe–Mg–Ca garnets.

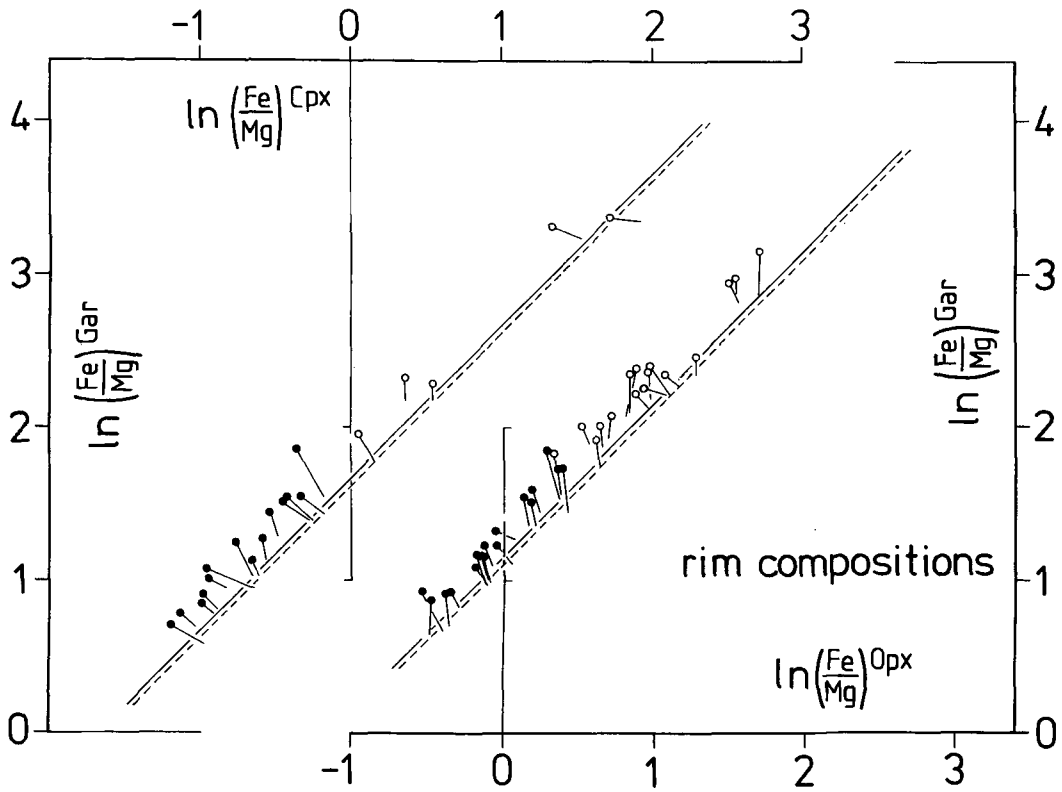

FIG. 9. Representation of Fe–Mg partitioning data (core compositions) for garnet–orthopyroxene and garnet–clinopyroxene pairs in $\ln(Fe/Mg)^{gar}$ *vs.* $\ln(Fe/Mg)^{pyx}$ diagrams. Circles—charnockites; dots—basic granulites. The small scatter of the data indicates cessation of retrograde Fe–Mg exchange at uniformly low temperatures. The stippled and continuous lines represent the partitioning trends for core compositions of isolated and contact phases respectively (see Fig. 8).

The $\ln K_{eFeMg^{-1}}^{Gar-Opx}$–$X_{Fe}$ relations shown in Fig. 13 illustrate the compositional effects of selected garnet solution models on the equilibrium constant. Surprisingly the compositional dependence of $\ln K_e$ is almost completely eliminated by a symmetric solution model for garnet (Hodges and Spear, 1982) in which only non-ideal mixing in the Ca–Mg and Ca–Fe binary joins (Newton *et al.*, 1977) is considered. In contrast, the asymmetric ternary solution model of Ganguly and Saxena (1984) which includes non-ideal Fe–Mg mixing terms deduced from regression analysis of natural partitioning data, yields a systematic compositional dependence of $\ln K_e$ over the whole range of X_{Fe} compositions. More recently, Chatterjee (1987), Berman (1990) and Bhattacharya *et al.* (1990) have refined the asymmetric ternary solution model by an improved evaluation of the mixing properties for the Ca–Mg, Ca–Fe and Fe–Mg binaries based on experimental phase-equilibrium and calorimetric data. However, since the evaluation of the mixing properties was based on different data sets and assumptions, there is little agreement between the models and consequently the $\ln K_e$–X_{Fe} relations are discrepant (Fig. 13): whereas the compositional dependence of Fe–Mg partitioning is almost completely eliminated by the solution model of Chatterjee (1987), the model of Bhattacharya *et al.* (1990) yields a slight dependence for the very Fe-rich compositions, and a strong compositional dependence of $\ln K_e$ over the whole X_{Fe} range is obvious for the model of Berman (1990). A straightforward valuation of the garnet solution models is not possible since the evaluation of the garnet mixing properties in addition to the data base is highly dependent on the solution model adopted for the coexisting phase. The $\ln K_e$–X_{Fe} relations for the Sri Lankan granulites suggest that the approximation of orthopyroxene as a two-site ideal solution by Chatterjee (1987) and Berman (1990), in agreement with calorimetric data (Chatillon-Colinet *et al.*, 1983; Sharma *et al.*, 1987), might not be

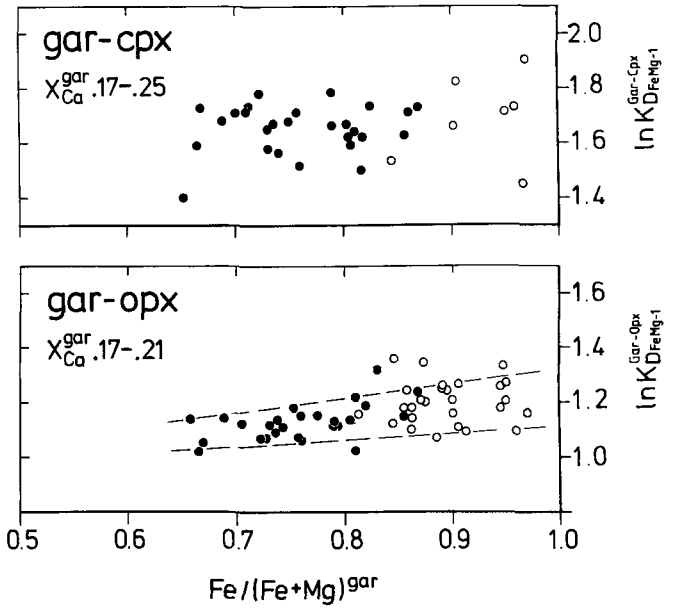

FIG. 10. Relationships between $\ln K_{DFeMg-1}$ for gar–opx and gar–cpx pairs and X_{Fe} bulk composition (expressed by Fe/(Fe + Mg)^{gar}). To avoid effects resulting from non-ideal Ca–Mg–(Fe) mixing in garnet, only samples with buffered garnet composition (X_{Ca} = 0.17–0.21 resp. 0.25) have been considered. The compositional dependence of $\ln K_{DFeMg-1}$ for the gar–opx pair indicates effects of non-ideal Fe–Mg mixing. For further discussion see text.

justified for the temperature range of granulite facies metamorphism (cf. Aranovich and Podlesskii, 1989; Bhattacharya *et al.*, 1990).

The results of *gar–cpx thermometry* are also highly discordant and span the wide temperature range from 640 to 1050 °C (Fig. 12). The relatively small spread of the temperature data, however, as in the case of gar–opx thermometry, indicates near-isothermal Fe–Mg equilibration of garnet and clinopyroxene throughout the studied terrane. As expected from the $\ln K_D$–X_{Fe} systematics (Fig. 10) which indicates cancellation of non-ideality effects in garnet and clinopyroxene, there exists no compositional dependence for temperature estimates obtained from those calibrations in which excess energy terms to account for non-ideal Fe–Mg mixing in the phases have been ignored (models of Råheim and Green, 1974; Ellis and Green, 1979; Krogh, 1988). It is evident that an artificial compositional dependence of the temperature data is created if in the calibration solely non-ideality in the garnet is considered (model of Dahl, 1980). Ganguly (1979) and Saxena (1979) in their calibrations of the gar–cpx thermometer have introduced complex yet not well contained activity models for the multicomponent garnet and clinopyroxene solid solutions which compensate the compositional effects on $\ln K_D$. The temperature data, however, do not necessarily prove the validity of the adopted solution models. The reversed experimental cation exchange data of Pattison and Newton (1989) in combination with a refined asymmetric solution model for the ternary Ca–Fe–Mg garnets should allow a refinement of the mixing model for the granulite clinopyroxenes, which is beyond the scope of this paper.

Control of mineral compositions by net-transfer reactions: the Fe,Mg–orthopyroxene + anorthite ⇌ (Fe,Mg)$_2$Ca–garnet + quartz equilibrium

For a precise evaluation of paleo-pressures recorded by the assemblages of garnet–pyroxene granulites with the opx + an ⇌ gar + qtz geobarometer, calibrations must be based on accurate *P–T* locations of the end member reactions in the CMAS resp. CFAS systems (cf. Perkins and Newton, 1981; Bohlen *et al.*, 1983; Berman, 1988; Holland and Powell, 1990), as well as adequate activity models for the participating phases.

At present, the major problems in the application of this geobarometer to granulite assemblages result from the incomplete knowledge of activity-composition relations of the multicomponent natural solid solutions. Since the mineral

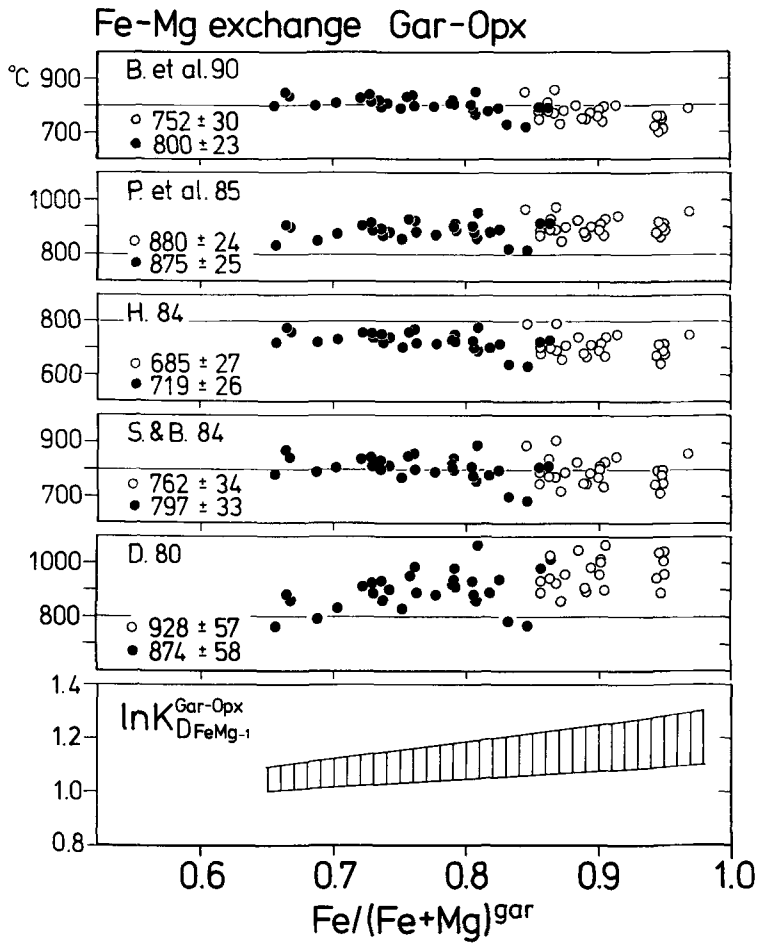

FIG. 11. Results of garnet–orthopyroxene Fe–Mg exchange thermometry (from bottom to top): Dahl, 1980; Sen and Bhattacharya, 1984; Harley, 1984; Perchuk *et al.*, 1985; Bhattacharya *et al.*, 1990. The core compositions of isolated phases or coarse-grained contact phases, which are considered to represent chemical equilibrium at near-peak granulite facies metamorphism, were used in the calculations. Although there is evidence of a regional pressure gradient in the order of 3–4 kbar, the temperatures have been calculated for a constant pressure value of 7 kbar. Circles—charnockites; dots—basic granulites. The T *vs.* Fe/(Fe + Mg)^{gar} diagrams reveal compositional effects on the T estimates for most of the calibrations which evidently indicates inappropriate modelling of the activity-composition relations for the coexisting phases.

assemblages of the charnockites and basic granulites equilibrated almost isothermally, the $\ln K_e$-data for the core compositions of isolated resp. coarse-grained mineral phases when based on correct activity models, should mirror the paleo-pressure regime. Alternatively, samples from small areas of defined tectonic position and identical P–T history might well be used to test the validity of the adopted activity models.

For a critical comparison of currently used garnet activity models, the $\ln K_e$-data for a selected set of samples inferred to have equilibrated at almost isothermal–isobaric conditions were calculated adopting a two-site ideal solution model for orthopyroxene and the activity formulations of Blencoe *et al.* (1982) for plagioclase. The graphical representation of the $\ln K_3$–X_{Fe} relations in Fig. 14 shows that the garnet solution models adopted in the calibrations of the barometer by Newton and Perkins (1982) and Perkins and Chipera (1985; modified asymmetric solution model of Ganguly and Saxena, 1984) obviously do not adequately correct for the compositional dependence of $\ln K_D$. For the extreme bulk compositions, the $\ln K_e$ data would indicate a difference of paleo-pressure in the

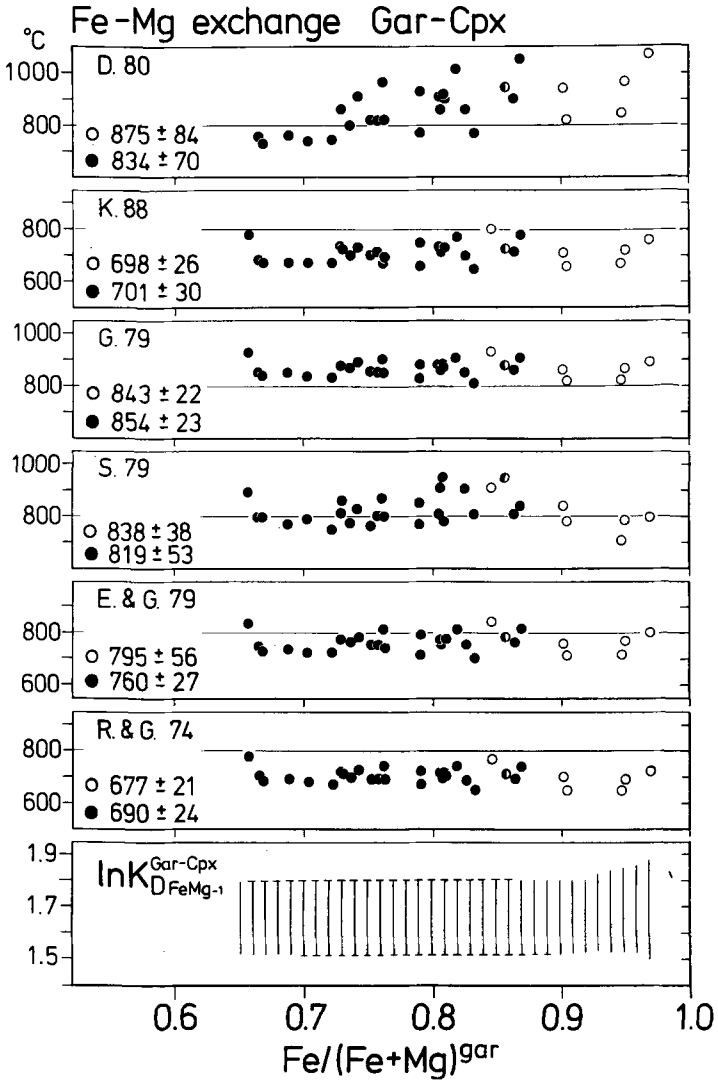

FIG. 12. Results of garnet–clinopyroxene Fe–Mg exchange thermometry (from bottom to top): Råheim and Green (1974), Ellis and Green (1979), Saxena (1979), Ganguly (1979), Krogh (1988), Dahl (1980). The core compositions of isolated phases or coarse-grained phases which are considered to represent chemical equilibrium at near-peak granulite facies metamorphism were used in the calculations. Despite of the regional pressure gradient in the order of 3–4 kbar, the temperature data were calculated for a constant pressure value of 7 kbar. Circles—charnockites; dots—basic granulites. Compositional dependences are obvious for some calibrations and reflect inadequate modelling of the activity-composition relations for the coexisting phases.

order of 2 kbar. Considerably smaller dependences of $\ln K_e$ on bulk X_{Fe} composition result for the recently refined garnet solution models (Chatterjee, 1987; Aranovich and Podlesskii, 1989; Berman, 1990; Bhattacharya *et al.*, 1990). The individual $\ln K_e$ data sets, however, differ considerably and would yield model-dependent pressure differences up to 4 kbar. The slight compositional dependence could imply that the approximation of orthopyroxene as a two-site ideal solution is not valid, at least for the temperature range <800 °C. If Fe–Mg orthopyroxenes would behave non-ideally also at higher temperatures, the recent refinements (Chatterjee, 1987; Berman, 1990) would not adequately constrain the garnet mixing properties on the

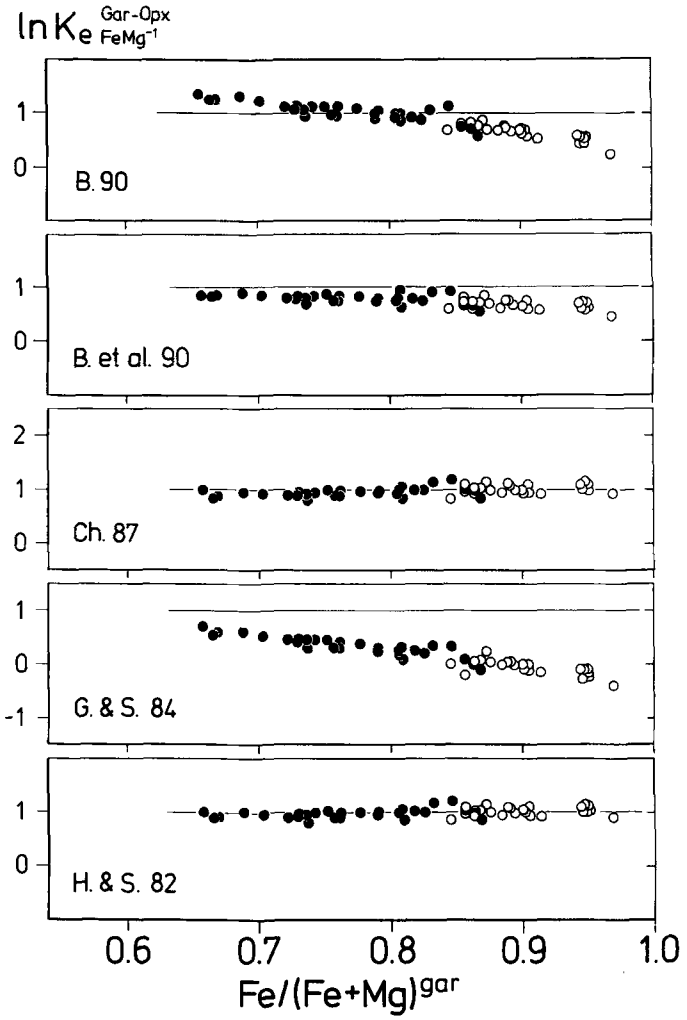

FIG. 13. Relationships between $\ln K_{eFeMg-1}$ for gar–opx pairs and X_{Fe} bulk composition (expressed by Fe/(Fe + Mg)^{gar}). To illustrate the compositional effects of different garnet solution models on the equilibrium constant, an ideal two-site mixing model for orthopyroxene was adopted in the computations. The following garnet solution models are compared (from bottom to top). Hodges and Spear (1982), Ganguly and Saxena (1984), Chatterjee (1987), Bhattacharya *et al.* (1990), Berman (1990).

Fe–Mg join and, in this case, would call for a complete reevaluation of the garnet mixing properties (cf. Bhattacharya *et al.*, 1990). This discussion presumes tacitly that the mixing properties of plagioclase are adequately described by the solution model of Blencoe *et al.* (1982).

The $\ln K_e$-formulation based on the garnet as well as orthopyroxene activity models of Bhattacharya *et al.* (1990) was used to examine the pressure-control on the compositions of coexisting mineral phases in the garnet–pyroxene granulites (Fig. 15). In the basic granulites, almandine and grossular contents in garnet, ferrosilite content in orthopyroxene and anorthite component in plagioclase decrease linearly with increasing pressure. The charnockites show a more complex compositional control by pressure: almandine content in garnet and anorthite component in plagioclase, similar to the trends observed in the basic granulites, decrease steadily with pressure. However, in the clinopyroxene-free assemblages characterizing the low-pressure regime ($\ln K_e = -1.8$ to -1.2), the grossular content increases with pressure essentially at the expense of the pyrope content until garnet

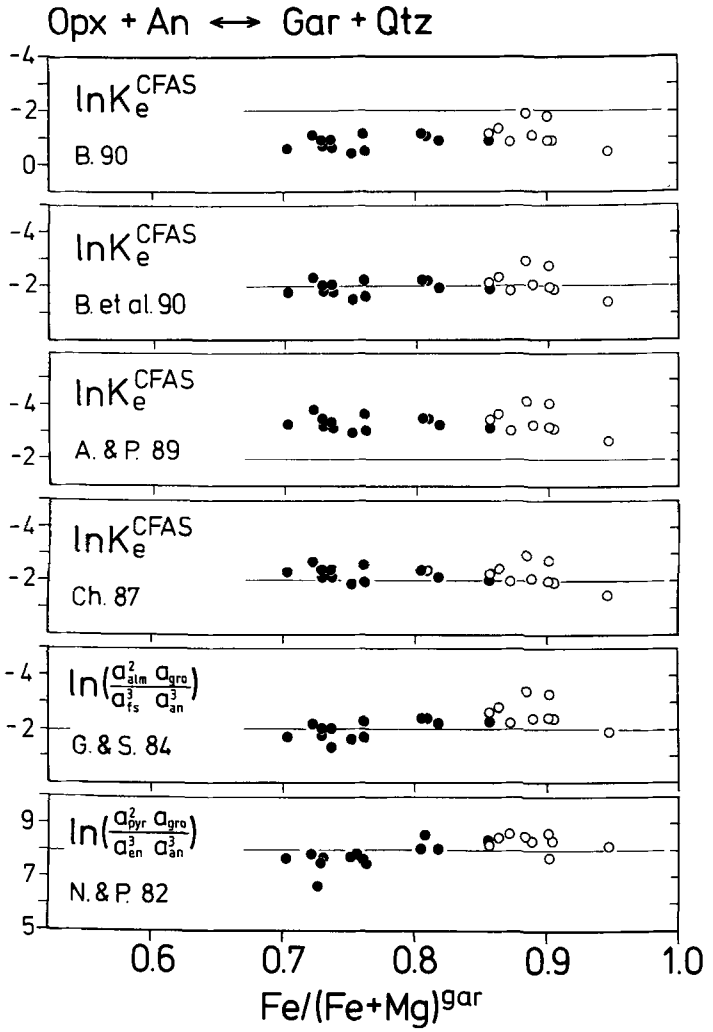

FIG. 14. Relations between $\ln K_e$ of the strongly pressure dependent reaction opx + an $\rightleftharpoons$ gar + qtz and the X_{Fe} bulk composition (expressed by Fe/(Fe + Mg)^{gar}). To examine the compositional effects of different garnet activity models on the equilibrium constant, only samples with identical P–T history were considered. An ideal two-site model was adopted for the orthopyroxene solid solution and the model of Blencoe *et al.* (1982) for plagioclase. The following garnet solution models are compared (from bottom to top): Newton and Perkins (1982; CMAS-system), Ganguly and Saxena (1984, CFAS-system), Chatterjee (1987), Aranovich and Podlesskii (1989), Bhattacharya *et al.* (1990), Berman (1990). Circles–charnockites; dots–basic granulites.

becomes saturated in Ca content which indicates the predominance of the strongly pressure sensitive reaction opx + an $\rightleftharpoons$ $(FeMg)_2Ca$–gar + qtz. This compositional development is accompanied by an increase in the ferrosilite component in orthopyroxene with pressure, so that the Fe–Mg distribution coefficient for the isothermally equilibrated mineral pair is adjusted. In the charnockite assemblages of the medium to high-pressure regimes, the compositional trends parallel those of the basic granulites.

The large variation in $\ln K_e$ indicates pronounced variations of paleo-pressure in the southern granulite terrane of Sri Lanka. To assess regional gradients, pressures were evaluated by combining the gar–opx Fe–Mg exchange geothermometer and the opx + plg $\rightleftharpoons$ gar + qtz geobarometer (calibrations by Bhattacharya

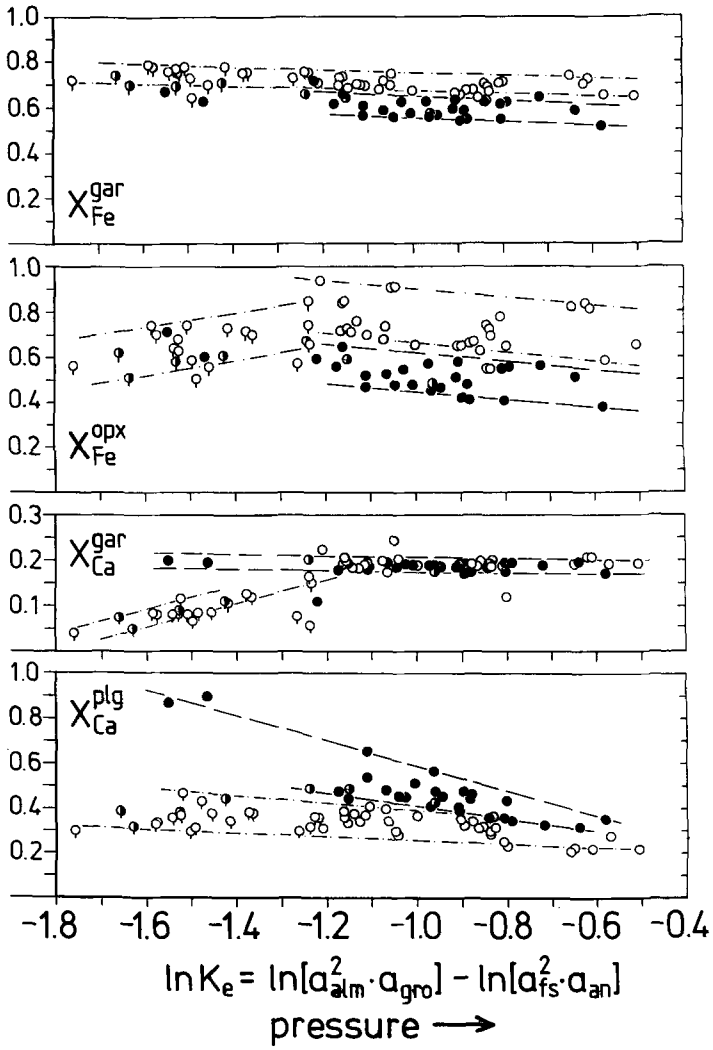

FIG. 15. Relationships between compositional parameters of coexisting phases (cores) and the $\ln K_e$ of the strongly pressure dependent net-transfer reaction opx + an ⇌ gar + qtz (CFAS system). Because of the near-isothermal equilibration of charnockites (circles) and basic granulites (dots), the diagram illustrates the systematic development of mineral compositions with increase in pressure.

et al., 1990). A graphical representation of the data reveals a systematic regional variation of paleo-pressure which correlates extremely well with the tectonic structure (Fig. 16). Highest pressures (>9 kbar) are recorded by granulites of the Highland Series occurring as inlayers and klippen within the amphibolite facies Eastern Vijayan basement. High pressures of 8–9 kbar characterize the structurally deepest units of the South-West Group and Highland Series close to the thrust contact with the Eastern Vijayan. Towards the higher tectonic levels in the west, the paleo-pressures decrease until, in the structurally highest synforms near the west coast, the lowest pressures (<5 kbar) are recorded.

Conclusions

One of the major problems in the application of geothermobarometry to natural assemblages is due to the fact that the activity–composition relations for the natural multi-component solid solutions are not well enough constrained. Generally, the thermochemical data are evalu-

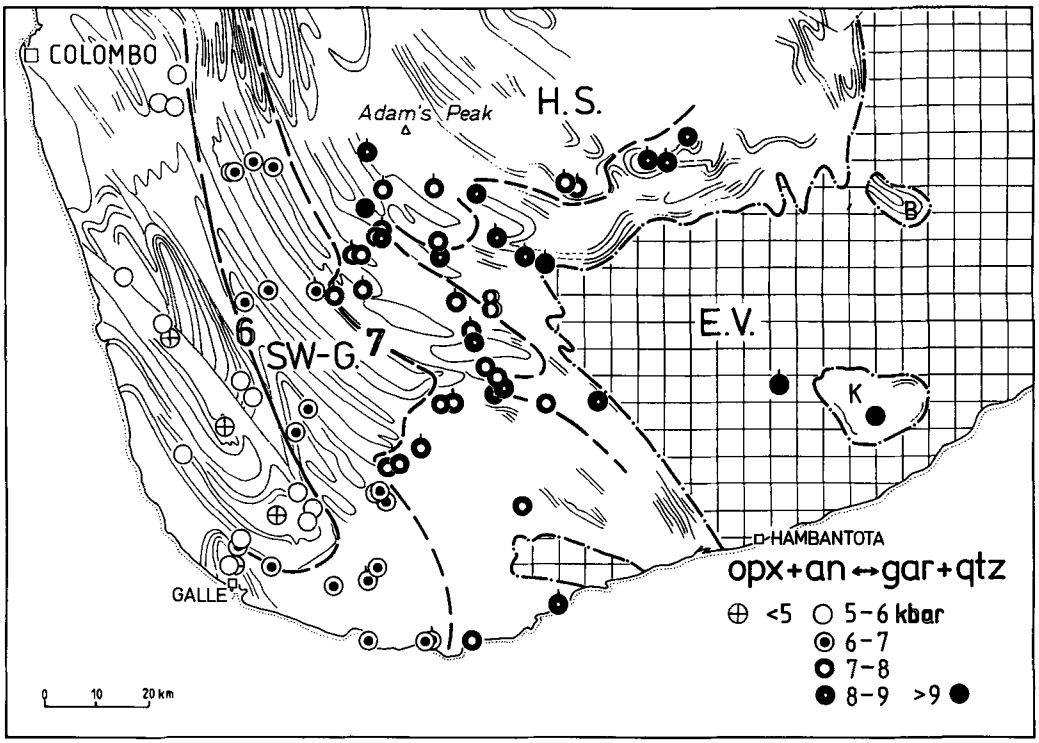

FIG. 16. Variation of paleo-pressure in the southern part of Sri Lanka based on P estimates evaluated by combination of the gar–opx Fe–Mg exchange thermometer with the opx + plg $\rightleftharpoons$ gar + qtz geobarometer (calibrations of Bhattacharya *et al.*, 1990). There is an excellent correlation of the pressure gradient with the tectonic structure.

ated from experimental mineral equilibrium data and calorimetric measurements for binary subsystems only (e.g. the Ca–Mg, Ca–Fe and Fe–Mg garnet binaries; cf. Berman, 1990) and for temperatures well beyond the thermal regime of the metamorphic assemblages. In principle, the mixing parameters for complex solid solutions could be evaluated from mineral chemistry data of well-equilibrated natural assemblages and precisely constrained P–T conditions of equilibration. A limitation of this approach lies in the difficulty in proving the equilibrium state between the mineral phases of an assemblage and in quantifying the P–T conditions of chemical equilibrium with reliable and independent methods.

The present study, however, shows that the garnet–pyroxene granulites of the central granulite belt in southern Sri Lanka are ideally suited for an investigation of these aspects: (1) the tectono–metamorphic history of the terrane is well constrained, (2) the mineral assemblages of garnet–pyroxene granulites preserve large-scale textural and chemical equilibrium attained during syn- to post-deformational wholesale recrystallization at conditions of the granulite facies, (3) near-isothermal chemical equilibration of the mineral phases within the entire terrane is documented by the Fe–Mg partitioning data, (4) the ferro-magnesian phases exhibit extreme variations in Fe–Mg composition, due to the highly variable bulk chemistry.

Application of commonly used calibrations of the gar–opx and gar–cpx Fe–Mg exchange thermometers and the opx + plg $\rightleftharpoons$ gar + qtz barometer to the Sri Lankan data set yields highly discordant P–T estimates and reveals more or less pronounced compositional dependences for all the tested calibrations. The results indicate that (1) the activity models for the involved phases as adopted in the calibrations do not adequately describe the mixing properties of the multi-component natural solid solutions and, (2) the ΔG° of the reactions, especially for the Fe–Mg exchange equilibria are not well enough constrained. A critical valuation of the different activity models for a specific phase (e.g. garnet) is not possible since the compositional dependences of the equilibrium constants reflect the bulk non-

ideality contributions and hence strongly depend on the solution model assumed for the involved coexisting phases (e.g. orthopyroxene, clinopyroxene, plagioclase). The refinemnt of activity models of specific phases based on the Sri Lankan data set would require the independent estimation of equilibrium P–T conditions and accurate descriptions of the mixing properties for the coexisting phases which both of which are not available at present.

From the comparison of the various geothermobarometric models it is suggested that (1) the currently favoured calibrations of the opx + plg $\rightleftharpoons$ gar + qtz barometer by Newton and Perkins (1982) and Perkins and Chipera (1985) should not be applied to granulites due to their strong compositional dependence. Instead, a calibration of the reactions (CMASH or CFASH systems) based on $\Delta G°$ derived from the internally consistent thermodynamic data sets of Berman (1988) or Holland and Powell (1990), a two-site ideal mixing model for orthopyroxene, the plagioclase solution model of Blencoe *et al.* (1982) and the asymmetric solution models for Ca–Fe–Mg garnets of Chatterjee (1987), Aranovich and Podlesskii (1989) or Bhattacharya *et al.* (1990) is recommended; (2) the gar–opx Fe–Mg exchange thermometer in the calibration of Bhattacharya *et al.* (1990) which also takes into account non-ideal Fe–Mg mixing in orthopyroxene should be preferred over the other models since it shows very little compositional dependence and yields temperature estimates which agree well with independent petrologic temperature constraints (Wo- and Scap-assemblages; gar–qtz oxygen isotope thermometry); (3) among the various tested calibrations of the gar–cpx Fe–Mg exchange thermometer, that of Ellis and Green (1979) yields the petrologically most reasonable temperature estimates.

Acknowledgements

To our colleagues of the German Sri Lanka consortium and our Sri Lankan colleagues Prof. P. W. Vitanage and W. K. B. N. Prame we convey thanks for the stimulating and constructive discussions and for the help during joint field work. The careful review by B. W. D. Yardley is greatly appreciated. This research would not have been possible without the financial support by the Deutsche Forschungsgemeinschaft.

References

Aranovich, L. Ya. and Podlesski, K. K. (1989) Geothermobarometry of high-grade metapelites: simultaneously operating reactions. In *Evolution of Metamorphic Belts* (Daly, J. S., Cliff, R. A., and Yardley, B. W. D., eds.) Geol. Soc. Spec. Publ., **43**, 45–61.

Berger, A. R. and Jayasinghe, N. R. (1976) Precambrian structure and chronology in the Highland Series of Sri Lanka. *Precambrian Res.*, **3**, 559–76.

Berman, R. G. (1988) Internally-consistent thermodynamic data for minerals in the system Na_2O–K_2O–CaO–MgO–FeO–Fe_2O_3–Al_2O_3–SiO_2–TiO_2–H_2O–CO_2. *J. Petrol.*, **29**, 445–552.

——(1990) Mixing properties of Ca–Mg–Fe–Mn garnets. *Am. Mineral.*, **75**, 328–44.

Bhattacharya, A., Krishnakumar, K., Raith, M., and Sen, S. K. (1990) An improved set of a–X parameters in Fe–Mg–Ca garnets and refinement of the orthopyroxene-garnet thermometer and the garnet–orthopyroxene–plagioclase–quartz barometer. Submitted to *J. Petrol.*

Blencoe, J. G., Merkel, G. A., and Seil, M. K. (1982) Thermodynamics of crystal–fluid equilibria, with applications to the system $NaAlSi_3O_8$–$CaAl_2Si_2O_8$–SiO_2–NaCl–CaCl–H_2O. In *Advances in Physical Geochemistry*, **2**, (Saxena, S. K., ed.), 191–223. Springer Verlag, New York.

Bohlen, S. R., Wall, V. J., and Boettcher, A. L. (1983) Experimental investigation and application of garnet granulite equilibria. *Contrib. Mineral. Petrol.*, **83**, 52–61.

Chatillon-Colinet, C., Newton, R. C., Perkins III, D., and Kleppa, O. J. (1983) Thermochemistry of $(Fe^{2+},Mg)SiO_3$ orthopyroxene. *Geochim. Cosmochim. Acta*, **47**, 1597–603.

Chatterjee, N. (1987) Evaluation of thermochemical data on Fe–Mg olivine, orthopyroxene, spinel and Ca–Fe–Mg–Al garnet. Ibid., **51**, 2515–25.

Cooray, P. G. (1978) Geology of Sri Lanka. In *Proceedings of the 3rd regional conference on geology and mineral resources of SE-Asia.* Bangkok, Thailand, 701–10.

Dahl, P. S. (1980) The thermal–compositional dependence of Fe^{2+}–Mg distributions between coexisting garnet and pyroxene: applications to geothermometry. *Am. Mineral.*, **65**, 854–66.

Ellis, D. J. and Green, D. H. (1979) An experimental study of the effect of Ca upon garnet-clinopyroxene Fe–Mg exchange equilibria. *Contrib. Mineral. Petrol.*, **71**, 13–22.

Faulhaber, S. (1991) *Die Granat-Pyroxen Granulite Süd-Sri Lankas: Petrologie und Geothermobarometrie*. Ph.D. Thesis, University of Bonn, FRG.

Fiorentini, E., Hoernes, S., Hoffbauer, R., and Vitanage, P. W. (1990) Nature and scale of fluid-rock exchange in granulite grade rocks of Sri Lanka: a stable isotope study. In *Granulites and Crustal Evolution* (Vielzeuf, D. and Vidal, Ph., eds.) NATO ASI Series, Series C, Vol. 311, 311–38.

Frost, B. R. and Chacko, T. (1989) The granulite uncertainty principle: limitations on thermobarometry in granulites. *J. Geol.*, **97**, 435–50.

Ganguly, J. (1979) Garnet and clinopyroxene solid solutions, and geothermometry based on Fe–Mg distribution coefficient. *Geochim. Cosmochim. Acta*, **43**, 1021–9.

——and Saxena, S. K. (1984) Mixing properties of aluminosilicate garnets: constraints from natural and experimental data, and applications to geothermobarometry. *Am. Mineral.*, **69**, 88–97.

Geiger, C. A., Newton, R. C., and Kleppa, O. J. (1987) Enthalpy of mixing of synthetic almandine-grossular and almandine-pyrop garnets from high temperature solution calorimetry. *Geochim. Cosmochim. Acta,* **51**, 1755–63.

Harley, S. L. (1984) An experimental study of the partitioning of Fe and Mg between garnet and orthopyroxene. *Contrib. Mineral. Petrol.*, **86**, 359–73.

Hodges, K. V. and Spear, F. S. (1982) Geothermometry, geobarometry and the Al_2SiO_5 triple point at Mt. Moosilauke, New Hampshire. *Am. Mineral.*, **67**, 1118–34.

Holland, T. J. B. and Powell, R. (1990) An enlarged and updated internally consistent thermodynamic dataset with uncertainties and correlations: the system K_2O–Na_2O–CaO–MgO–MnO–FeO–Fe_2O_3–Al_2O_3–TiO_2–SiO_2–C–H_2O–O_2. *J. Metamorph. Geol.*, **8**, 89–124.

Hölzl, S. and Köhler, H. (1989) U-Pb-Geochronologie an Unterkrustengesteinen Sri Lankas. *Europ. J. Mineral.*, **1**, 75.

Katz, M. B. (1971) The Precambrian metamorphic rocks of Ceylon. *Geol. Rundschau,* **60**, 1523–49.

Krogh, E. J. (1988) The garnet–clinopyroxene Fe–Mg geothermometer—a reinterpretation of existing experimental data. *Contrib. Mineral. Petrol.*, **99**, 44–8.

Milisenda, C. C., Liew, T. C., Hofmann, A. W., and Kröner, A. (1988) Isotopic mapping of age provinces in Precambrian high-grade terrains: Sri Lanka. *J. Geol.*, **96**, 608–15.

Newton, R. C. and Perkins III, D. (1982) Thermodynamic calibration of geobarometers based on the assemblages garnet–plagioclase–orthopyroxene (clinopyroxene)-quartz. *Am. Mineral.*, **67**, 230–22.

——Charlu, T. V., and Kleppa, O. J. (1977) Thermochemistry of high pressure garnets and clinopyroxenes in the system CaO–MgO–Al_2O_3–SiO_2. *Geochim. Cosmochim. Acta,* **41**, 369–77.

Pattison, D. R. M. and Newton, R. C. (1989) Reversed experimental calibration of the garnet–clinopyroxene Fe–Mg exchange thermometer. *Contrib. Mineral. Petrol.*, **101**, 87–103.

Perchuk, L. L., Aranovich, L. Ya., Podlesskii, K. K., Lavrant'eva, I. V., Gerasimov, V. Yu., Fed'kin, V. V., Kitsul, V. I., Karsakov, L. P., and Berdnikov, N. V. (1985) Precambrian granulites of the Aldan shield, eastern Siberia, U.S.S.R. *J. Metamorph. Geol.*, **3**, 265–310.

Perkins, III, D. and Chipera, S. J. (1985) Garnet–orthopyroxene–plagioclase–quartz barometry: refinement and application to the English River subprovince and the Minnesota River valley. *Contrib. Mineral. Petrol.*, **89**, 69–80.

——and Newton, R. C. (1981) Charnockite geobarometers based on coexisting garnet–pyroxene–plagioclase–quartz. *Nature*, **292**, 144–6.

Powell, R. and Holland, T. J. B. (1985) An internally consistent thermodynamic dataset with uncertainties and correlations: 1. Methods and a worked example. *J. Metamorph. Geol.*, **3**, 327–42.

Råheim, A. and Green, D. H. (1974) Experimental determination of the temperature and pressure dependence of the Fe–Mg partition coefficient for coexisting garnet and clinopyroxene. *Contrib. Mineral. Petrol.*, **48**, 179–203.

Sandiford, M., Powell, R., Martin, S. F., and Perera, L. R. K. (1988) Thermal and baric evolution of garnet granulites from Sri Lanka. *J. Metamorph. Geol.*, **6**, 351–64.

Saxena, S. K. (1979) Garnet–clinopyroxene geothermometer. *Contrib. Mineral. Petrol.*, **70**, 229–35.

Schumacher, R., Schenk, V., Raase, P., and Vitanage, P. W. (1990) Granulite facies metamorphism of metabasic and intermediate rocks in the Highland Series of Sri Lanka. In *High-grade metamorphism and crustal anatexis* (Ashworth, J. R. and Brown, M., eds.) Allan & Unwin, London.

Selverstone, J. and Chamberlain, C. P. (1990) Apparent isobaric cooling paths from granulites: two counterexamples from British Columbia and New Hampshire. *Geology,* **18**, 307–10.

Sen, S. K. and Bhattacharya, A. (1984) An orthopyroxene–garnet thermometer and its application to the Madras charnockites. *Contrib. Mineral. Petrol.*, **88**, 64–71.

Sharma, K. C., Agrawal, R. D., and Kapoor, M. L. (1987) Determination of thermodynamic properties of (Fe–Mg)-pyroxenes at 1000 K by the emf method. *Earth Planet. Sci. Lett.*, **85**, 302–10.

Vitanage, P. W. (1985) The geology, structure and tectonics of Sri Lanka and South India. In *Recent Advances in the Geology of Sri Lanka* (Dissanayake, C. B. and Cooray, P. G., eds.) Centre international pour la formation et les échanges géologiques, CIFEG. Publication occasionalle No. 6, 5–15.

[*Revised manuscript received 5 September 1990*]